Convergent functional effects of antidepressants in major depressive disorder: a neuroimaging meta-analysis

Amin Saberi[1,2,3], Amir Ebneabbasi[4,5], Sama Rahimi[1,2,6], Sara Sarebannejad[7], Zumrut Duygu Sen[8,9,10,11], Heiko Graf[12], Martin Walter[8,9,10,13], Christian Sorg[14,15,16], Julia A. Camilleri[1,2], Angela R. Laird[17], Peter T. Fox[18], Sofie L. Valk[1,2,3], Simon B. Eickhoff[1,2], Masoud Tahmasian[1,2,19]

[1] Institute of Neurosciences and Medicine (INM-7), Research Centre Jülich, Jülich, Germany.
[2] Institute of Systems Neuroscience, Heinrich Heine University Düsseldorf, Düsseldorf, Germany.
[3] Otto Hahn Research Group for Cognitive Neurogenetics, Max Planck Institute for Human Cognitive and Brain Sciences, Leipzig, Germany
[4] Department of Clinical Neurosciences, University of Cambridge, Biomedical Campus, Cambridge CB2 0QQ, UK.
[5] Cambridge University Hospitals NHS Trust, Cambridge CB2 0SZ, UK.
[6] Neuroscience Center, Goethe University, Frankfurt, Hessen, Germany.
[7] Kavli Institute for Systems Neuroscience, Norwegian University of Science and Technology, Trondheim, Norway.
[8] Department of Psychiatry and Psychotherapy, University Hospital Jena, Jena, Germany.
[9] Clinical Affective Neuroimaging Laboratory (CANLAB), Magdeburg, Germany.
[10] Department of Psychiatry and Psychotherapy, University Tübingen, Tübingen, Germany.
[11] German Center for Mental Health, Halle-Jena-Magdeburg, DZP, Germany.
[12] Department of Psychiatry and Psychotherapy III, University of Ulm, Ulm, Germany.
[13] Leibniz Institute for Neurobiology, Brenneckestr. 6, 39118 Magdeburg, Germany.
[14] TUM-Neuroimaging Center (TUM-NIC), Klinikum Rechts der Isar, Technische Universität München, Munich, Germany.
[15] Department of Neuroradiology, Klinikum Rechts der Isar, Technische Universität München, Munich, Germany.
[16] Department of Psychiatry and Psychotherapy, Klinikum Rechts der Isar, Technische Universität München, Munich, Germany.
[17] Department of Physics, Florida International University, Miami, FL, USA.
[18] University of Texas Health Science Center at San Antonio, San Antonio, TX, USA.
[19] Department of Nuclear Medicine, University Hospital and Medical Faculty, University of Cologne, Cologne, Germany.

* **Corresponding author:** Masoud Tahmasian M.D., Ph.D., Institute of Neuroscience and Medicine, Brain & Behaviour (INM-7), Research Centre Jülich, Wilhelm-Johnen-Straße, Jülich, Germany. Telefon: +49 2461 61-8785, Fax: +49 2461 61-1880. Email: m.tahmasian@fz-juelich.de

Running title: Meta-analytic functional effects of antidepressants in depression

Abstract

Background: Neuroimaging studies have provided valuable insights into the macroscale impacts of antidepressants on brain functions in patients with major depressive disorder. However, the findings of individual studies are inconsistent. Here, we aimed to provide a quantitative synthesis of the literature to identify convergence of the reported findings at both regional and network levels and to examine their associations with neurotransmitter systems.

Methods: Through a comprehensive search in PubMed and Scopus databases, we reviewed 5,258 abstracts and identified 36 eligible functional neuroimaging studies on antidepressant effects in major depressive disorder. Activation likelihood estimation was used to investigate regional convergence of the reported foci of consistent antidepressant effects, followed by functional decoding and connectivity mapping of the convergent clusters. Additionally, utilizing group-averaged data from the Human Connectome Project, we assessed convergent resting-state functional connectivity patterns of the reported foci. Next, we compared the convergent circuit with the circuits targeted by transcranial magnetic stimulation (TMS) therapy. Last, we studied the association of regional and network-level convergence maps with selected neurotransmitter receptors/transporters maps.

Results: No regional convergence was found across foci of treatment-associated alterations in functional imaging. Subgroup analysis across the Treated > Untreated contrast revealed a convergent cluster in the left dorsolateral prefrontal cortex, which was associated with working memory and attention behavioral domains. Moreover, we found network-level convergence of the treatment-associated alterations in a circuit more prominent in the frontoparietal areas. This circuit was co-aligned with circuits targeted by "anti-subgenual" and "Beam F3" TMS therapy. We observed no significant correlations between our meta-analytic findings with the maps of neurotransmitter receptors/transporters.

Conclusion: Our findings highlight the importance of the frontoparietal network and the left dorsolateral prefrontal cortex in the therapeutic effects of antidepressants, which may relate to their role in improving executive functions and emotional processing.

Introduction

Major depressive disorder (MDD) is the most common psychiatric disorder and a leading cause of disability worldwide [1]. Despite decades of research and the development of various pharmacological, psychological, and stimulation-based therapy, optimal treatment of MDD remains a challenge [2]. The conventional antidepressant medications, which are the mainstay of MDD treatment, can only achieve clinical response after several weeks of treatment [3] and only in around half the patients [4]. The challenges in the treatment of MDD are partly due to our limited understanding of the mechanisms by which antidepressants interact with the complex and heterogeneous neurobiology of MDD.

The monoamine neurotransmitter hypothesis of MDD postulates that decreased levels of serotonin and norepinephrine in specific brain regions are responsible for depressive symptoms, and antidepressant medications can normalize the imbalance in neurotransmitter levels [5]. While this hypothesis has dominated the field of MDD research and treatment for decades, it is increasingly being questioned, as the supporting evidence for a decreased concentration/activity of serotonin in MDD has been found inconclusive [6]. This, together with the discovery of rapid antidepressant effects of ketamine, a glutamate receptor antagonist [7, 8], suggests that the therapeutic effects of antidepressants cannot be simply explained as rebalancing the synaptic levels of the monoamine neurotransmitters. Thus, it is crucial to study the macroscale effects of antidepressant medications on the brain regions and networks beyond their neurochemical and cellular effects. Understanding these macroscale effects may help better understand their clinical effects on various symptoms of MDD, which is ultimately needed to improve treatment outcomes.

Neuroimaging techniques such as functional magnetic resonance imaging (fMRI) and positron emission tomography (PET) have been used to study the macroscale effects of antidepressants on brain activity, metabolism, or connectivity [9, 10]. These studies have reported diverse functional effects of antidepressants on various brain areas, such as: i) normalizing reactivity of the amygdala, insula, and anterior cingulate cortex to negative stimuli [11–14], ii) reducing metabolism of paralimbic and subcortical areas, paralleled by increasing metabolism of fronto-parietal areas [15], or iii) modulation of resting-state function in the frontal, limbic and occipital areas as well as basal ganglia [16–18]. However, while individual neuroimaging studies are useful, the breadth of the literature and inconsistencies among the reported findings [10], necessitates a quantitative synthesis of the published literature to identify the most consistent findings that are robust to the large variability of the individual studies (in terms of clinical features and methodology), as well as their susceptibility to false positive/negative effects due to the usually small samples [19, 20].

Neuroimaging meta-analysis is a promising tool that enables a quantitative synthesis of the previously published literature [21, 22]. The most common approach in neuroimaging meta-analyses, i.e., coordinate-based meta-analysis (CBMA), aims to find potential regional convergence across the peak coordinates of the reported effects in individual studies [23]. Several neuroimaging meta-analyses have previously used this approach to study the regional convergence of the brain effects associated with the treatment of MDD, focusing on various therapeutic approaches and different neuroimaging modalities [24–30]. However, MDD is increasingly being recognized as a brain network disorder with distributed abnormalities across

the whole brain, and similarly, the antidepressants' effects could be distributed across the brain rather than localized [9]. Such distributed effects may be overlooked by the CBMA approaches, which are inherently intended for regional localization of effects. Recently, a novel meta-analytic approach has been introduced which aims to identify the convergence of reported findings at the level of networks by characterizing the normative convergent connectivity of the reported foci tested against random foci [31]. Using this approach, it was shown that despite a lack of regional convergence of reported abnormalities in MDD [32], there is a convergence of their connectivity in circuits which recapitulates clinically meaningful models of MDD [31].

Here, we aimed to identify how the findings of the previous functional neuroimaging studies on the effects of antidepressants converge on both regional and network levels by performing an updated CBMA as well as a network-level meta-analysis on the reported findings. Following, we compared our meta-analytic findings with the targets of transcranial magnetic stimulation (TMS) therapy and their associated circuits. Last, we asked whether the pattern of the observed meta-analytic effects of antidepressant medications on functional imaging can be potentially explained by the regional distribution of the neurotransmitter receptors/transporters (NRT) linked to these medications, leveraging the publicly available PET maps of neurotransmitter receptors and transporters [33].

Methods

This meta-analysis was performed according to the best-practice guidelines for neuroimaging meta-analyses [21, 22] and is reported adhering to the Preferred Reporting Items for Systematic Reviews and Meta-Analyses (PRISMA) statement [34]. The protocol for this study was pre-registered on the International Prospective Register of Systematic Reviews (PROSPERO, CRD42020213202).

Search and study selection

We searched the PubMed and Scopus databases to identify peer-reviewed eligible neuroimaging studies investigating the effects of antidepressants on MDD. The search was performed in July 2022, using the keywords reported in Table S1. In addition, we searched the BrainMap annotated database of neuroimaging experiments using Sleuth by setting the diagnosis to MDD and pharmacology to the antidepressants [35–38]. Further, to avoid missing any additional relevant studies, we traced the references of relevant neuroimaging reviews/meta-analyses. Next, the duplicated records were removed, and the resulting 5258 unique records were assessed for eligibility by two raters (S.RJ. and S.SN.) independently. The eligibility of records was assessed first using their titles or abstracts and then, for the potentially relevant records, by examining their full texts. Other authors (A. E., A. S., M. T.) resolved any disagreements between the main raters.

As suggested previously [21, 22], original studies were included if: 1) they studied patients with MDD, excluding patients with other major psychiatric or neurological comorbidities and adolescent or late-life patients, 2) the patients were treated with antidepressants, 3) the antidepressants effects on the function of gray matter structures were investigated using eligible neuroimaging modalities, i.e., functional magnetic resonance imaging

(including task-based [tb-fMRI], resting-state [rs-fMRI] and arterial spin labeling [ASL-fMRI]), fluorodeoxyglucose positron emission tomography (FDG-PET), or single-photon emission computed tomography (SPECT), 4) the results of pre- vs. post-treatment, treated vs. placebo/untreated, or group-by-time interaction contrasts were reported as peak coordinates of significant clusters in standard spaces (Montreal Neurological Institute [MNI] or Talairach) or were provided by the authors at our request, 5) the analysis was performed across the whole brain, was not limited to a region of interest (ROI) or hidden ROI conditions such as small volume correction (SVC), as these approaches are biased toward finding significance in the respective areas, hence violating the assumption of ALE method that all voxels of the brain have a unified chance of being reported [21, 22], and 6) at least six subjects were included in each group (Fig. 1).

Data extraction and preprocessing

From the eligible studies, we extracted demographic and clinical data (number of participants, age, sex, response to treatment, medications, treatment duration), methodological details (imaging modality, scanner field strength, task paradigm, software package, statistical contrast, and the multiple comparisons correction method), as well as the peak coordinates/foci (x, y, z) of experiments' findings. Of note, we use the term "study" to refer to an individual publication, and the term "experiment" to refer to the individual group-level contrasts reported within each "study" (e.g., Treated > Untreated). Following the data extraction, the coordinates reported in Talairach space were transformed into MNI space [39], so that all the experiments are in the same reference space. If the applied reference space was not explicitly reported or provided by authors after our request, we assumed the default settings of the software packages were used for normalization [21, 22]. In addition, to avoid spurious convergence over the experiments performed on the same/overlapping samples (reported within or across studies), in each meta-analysis, we merged the coordinates from multiple experiments pertaining to the same/overlapping samples, to make sure that each study contributes once per analysis, as suggested previously [21, 22, 40].

Activation likelihood estimation

The revised version of the activation likelihood estimation (ALE) method [23] was used to test the regional convergence of the reported differences against the null hypothesis of randomly distributed findings across the brain. In this method, the peak coordinates were convolved with 3D Gaussian probability distributions that have a full width at half maximum, inversely proportional to the sample size. This allowed experiments with larger samples to have a greater statistical certainty in the meta-analysis. Next, for each experiment, the convolved foci were combined to generate per-experiment "modeled activation" (MA) maps. Subsequently, the MA maps for all the experiments included in the meta-analysis were combined into an ALE score map, representing the regional convergence of results at each location of the brain. The ALE score map was then statistically tested against a null distribution reflecting randomly distributed findings to distinguish true convergence from by-chance overlap [23, 40]. The resulting p-values were subsequently thresholded at voxel height threshold of $p < 0.001$. Finally, to avoid spurious findings [23], the resulting p-values were corrected for multiple comparisons using the family-wise error correction at the cluster level (cFWE). Specifically, the significance of cluster extents was assessed against a null distribution of maximum cluster sizes

generated using a Monte Carlo approach with 10,000 permutations, wherein for each permutation ALE was performed on randomly selected foci distributed across the grey matter, and the maximum size of resulting null clusters were recorded.

In addition to an ALE meta-analysis on all included experiments (the 'all-effects' ALE) we performed several complementary ALE meta-analyses based on the direction of the effect (treatment contrast i.e., Treated > Untreated [Tr+] or Untreated > Treated [Tr-]), imaging modality, study design, and type of the antidepressants. The analyses were performed only if 12 or more experiments were included in each category, as ALE analyses with too few experiments are likely to be largely driven by a single experiment and, therefore, lack sufficient statistical power to provide valid results [41].

Contribution assessment of the convergent clusters

For each significant convergent cluster, the relative contribution of included experiments was calculated as the fraction of the ALE values within the cluster accounted for by each experiment contributing to the cluster. Specifically, the contribution of each experiment to the cluster was calculated as follows: (i) Voxel-wise ratios were calculated between ALE score values of the cluster voxels after removing each experiment compared to the original ALE score calculated based on all included experiments. (ii) These ratios were averaged across the cluster voxels and subtracted from one, reflecting on average how much each experiment accounts for the ALE scores within the cluster. (iii) Contributions were normalized to a sum of 100%. Subsequently, we reported the contributions per categories of the contributing experiments according to modality, condition (task-based or resting-state), and medications, by summing up the contribution of the experiments within each category.

Functional decoding of the convergent clusters

We applied the data from task-based functional neuroimaging experiments and their annotated behavioral domains (BD) included in the BrainMap database [35–38] to identify BDs significantly associated with the convergent clusters identified in the main ALE analyses [42]. In particular, we used binomial tests to assess whether the probability of each cluster activation given a particular BD, i.e., P(Activation | BD), is significantly higher than the overall a priori chance of its activation across all BDs, i.e., P(Activation). The resulting p-values were subsequently adjusted for multiple comparisons at false discovery rate (FDR) of 5%.

Meta-analytic coactivation mapping of the convergent clusters

We investigated the task-based functional connectivity of the convergent clusters identified in the main ALE analyses using meta-analytic coactivation mapping (MACM) [43]. We used the data from task-based functional neuroimaging experiments on healthy individuals included in the BrainMap database [35–38]. For each identified convergence cluster from the main ALE analyses, we identified all the experiments that reported at least one focus of activation therein, and after merging the experiments reported within each study, performed an ALE meta-analysis across those studies, thresholded at $p_{cFWE} < 0.05$. This approach identifies brain regions consistently co-activated with the convergent cluster across all task-based functional neuroimaging experiments.

Resting-state functional connectivity of the convergent clusters

We obtained the group-averaged dense resting-state functional connectivity (RSFC) matrix of the Human Connectome Project – Young Adults (HCP- YA) dataset (n=1003) available in *Cifti* format [44, 45]. The convergent cluster in the MNI space was transformed to *fsLR* space using

neuromaps [46] and in turn mapped to *Cifti* 'grayordinates' (cortical vertex or subcortical voxel) covering the cluster extent. Subsequently, the whole-brain RSFC maps of these grayordinates were extracted from the HCP dense RSFC and were uniformly averaged, resulting in a RSFC map of the convergent cluster.

Network-based meta-analysis

In addition to the conventional CBMA, we performed a network-based meta-analysis approach [31], to identify convergent functional connectivity of the reported foci compared to randomly distributed foci. We used the normative group-averaged dense RSFC matrix of the HCP dataset in these analyses. For the given set of experiments in the all-effects, Tr+ and Tr- analyses, we performed the following: (i) The MNI coordinates of all the reported foci in the included experiments were mapped from the voxel space to their closest grayordinate based on Euclidean distance. The foci with no grayordinate in their 10 mm radius were excluded (16 out of 528). Of note, the median distance of the mapped grayordinates from the MNI coordinates of foci was 2.26 mm. (ii) The whole-brain RSFC maps of the foci were extracted from the HCP dense RSFC and averaged in two levels: First, the RSFC maps of the foci from each experiment were averaged across the foci to create average experiment-specific RSFC maps. Second, average experiment-specific RSFC maps were averaged across experiments, weighted by their sample sizes, which resulted in a pooled RSFC map of all the experiments included in the analysis. (iii) This observed RSFC map was compared to a permutation-based null distribution of RSFCs to create a Z-scored convergent connectivity map. Specifically, in each of the 1000 permutations, we randomly sampled an equal number of foci as reported in the included experiments and averaged their RSFC maps as described above in step ii, resulting in a set of 1000 null RSFC maps. (iv) We calculated two-tailed p-values as the frequency of null pooled RSFC exceeding the observed pooled RSFC at each grayordinate, and subsequently transformed the p-values to Z scores. These maps, referred to as 'convergent connectivity maps', reflect greater- or lower-than-chance connectivity of the reported foci to the rest of the brain, which indicate convergent circuits connected to the locations of reported antidepressant treatment effects. Of note, to assess the effect of weighting the second-level average by experiment sample sizes, we additionally performed a sensitivity analysis in which this weighting was not applied.

Using a similar approach, we additionally assessed convergent connectivity of the reported foci to the seven canonical resting-state networks [47]. Here, we averaged the true and null pooled RSFC maps (calculated in steps ii and iii above) within each network. Following, for each of the seven networks, a two-tailed p-value was calculated as the frequency of null within-network average of pooled RSFC exceeding that of the true foci. Lastly, we corrected for multiple comparisons across the seven networks by FDR adjustment at 5%.

Association with transcranial magnetic stimulation targets

We compared the location of the ALE convergent clusters with four TMS target coordinates, including the anatomical "5-CM" site (MNI -41, 16, 54) [48], "Beam F3" site (MNI -41, 42, 34) [49] and the "anti-subgenual" site (MNI –38, 44, 26) [50] used in clinical trials. In addition, we extracted the RSFC maps of grayordinates corresponding to these coordinates from the HCP dense RSFC and evaluated their spatial correlations with the all-effects convergent connectivity map of antidepressant effects as well as the RSFC maps of ALE convergent clusters.

In these correlations we parcellated the maps using Schaefer-400 parcellation in the cortex (400 parcels) and Tian S2 parcellation in the subcortex (32 parcels), and accounted for spatial autocorrelation by using permutation testing of variogram-based surrogated maps. In this approach, random surrogate maps were created with variograms that were approximately matched to that of the original map, as implemented in *BrainSMASH* [51]. Following, the Pearson correlation coefficient between observed maps X and Y was compared against a non-parametric null distribution of coefficients resulting from correlating surrogates of X with the observed map Y. Lastly, we corrected for multiple comparisons across the correlations using FDR adjustment at 5%. Notably, these associations were performed between parcellated maps given high computational costs of generating variogram-based surrogate maps at the level of grayordinates.

Association of meta-analytic findings with neurotransmitter receptor/transporter densities

The PET maps of tracers associated with NRT were obtained from a previous study [33], which curated these maps from various sources [52–69]. These maps were based on tracers for serotoninergic and noradrenergic receptors/transporters (5HT1a, 5HT1b, 5HT2a, 5HT4, 5HT6, 5HTT, NAT) as well as the NMDA receptor. The PET maps were available in MNI volumetric space and were parcellated using Schaefer-400 parcellation in the cortex (400 parcels) and Tian S2 parcellation in the subcortex (32 parcels), and were subsequently Z-scored across parcels. In case multiple maps were available for a NRT we calculated an averaged map weighted by the sample size of the source studies.

We then calculated the correlation of parcellated NRT maps with the all-effects convergent connectivity map while accounting for spatial autocorrelation by using variogram-based permutation testing as described above. In addition, we tested for over-/under-expression of the NRTs in the ALE convergent clusters. To do so, we first normalized the Z-scored and parcellated maps of NRTs to 0-1 and after projecting them to the cortical surface, calculated the median normalized density of each NRT within the convergent cluster. Next, we compared the observed median densities against a null distribution calculated based on surrogate NRT maps with preserved spatial autocorrelation which were generated using *BrainSmash* [51]. In all tests, the resulting p-values were corrected for multiple comparisons across the NRT maps by using FDR adjustment at 5%.

Data and code availability

The code used in this study can be accessed in a GitHub repository at https://github.com/amnsbr/antidepressants_meta. This repository includes all the Python code used to run the analyses and generate the figures apart from the MATLAB code used for behavioral decoding, which is available upon request. In addition, the repository includes the coordinates and processed data reported in our study, with the exception of: i) HCP-YA dense connectome is accessible to registered users at https://db.humanconnectome.org/, and ii) BrainMap dataset which is available as a file upon request, but is additionally searchable using Sleuth (https://www.brainmap.org/sleuth/).

Results

Experiments included in the meta-analysis

The study selection process is depicted in Fig. 1. We screened 5258 records resulting from our broad and sensitive search and assessed 586 full texts for eligibility to finally include 36 studies and 30 experiments with non-overlapping samples (Table 1 and Table S2) [12–18, 70–98]. Collectively 848 MDD patients were included in the experiments. The patients were treated using SSRIs (n=17), ketamine (n=7), SNRIs (n=7), mirtazapine (n=2), clomipramine (n=1), quetiapine (n=1), or bupropion (n=1). In six experiments, the patients received variable medications. The imaging modalities included were tb-fMRI (n=18), FDG-PET (n=4), H2O-PET (n=1), rs-fMRI (n=4), ASL-fMRI (n=2) and ^{99m}Tc-HMPAO SPECT (n=2).

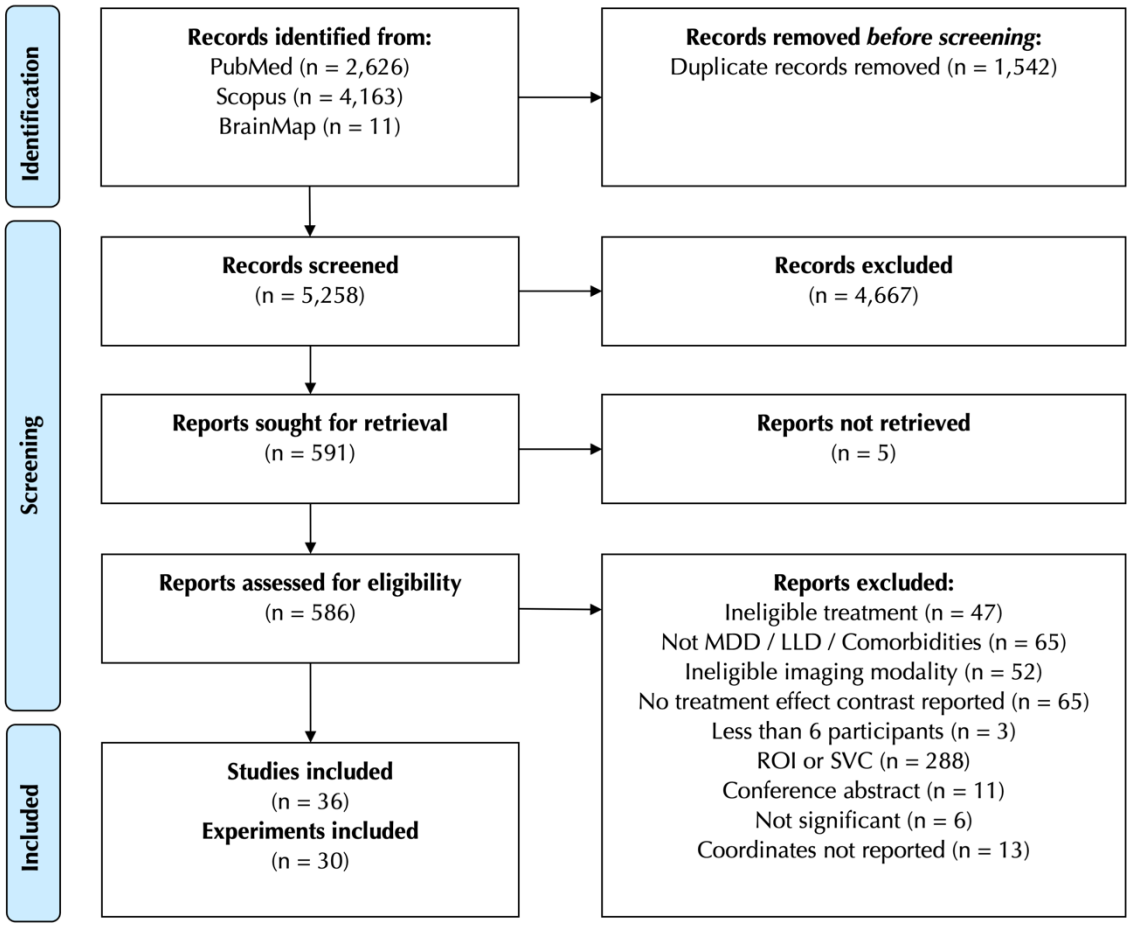

Fig. 1. Study selection flowchart.
MDD: major depressive disorder, LLD: late-life depression, ROI: region of interest, SVC: small volume correction.

Convergent regional effects of antidepressants

No statistically significant regional convergence was found in our ALE meta-analysis on all included experiments reflecting treatment-related alterations in brain function ($p_{cFWE} > 0.387$),

nor in its subgroup analyses limited to specific types of treatments or modalities (Table 2). However, among the Tr+ experiments (n=20) we observed a significant cluster of convergence in the left middle frontal gyrus within the dorsolateral prefrontal cortex (DLPFC) (MNI -38, 30, 28; 132 voxels) (Fig. 2). The convergence in this cluster was driven by contributions from seven experiments from eight studies [15, 17, 81–84, 86, 97]. The relative contribution of experiments using different medications included SSRIs (58.3%), ketamine (25.3%), and variable classes (16.4%). The contribution of experiments using PET (56.3%) was the highest, followed by fMRI (43.4%) and SPECT (0.3%). The scanning paradigms of contributing experiments included resting-state (81.0%) and emotional tasks (18.9%). Following, we investigated regional convergence of the Tr+ experiments across more specific subgroups of these experiments and found additional/different clusters (Fig. S1). To assess the convergence across classic antidepressants, we performed a subgroup analysis after excluding ketamine among 14 Tr+ experiments and found clusters of convergence in the left (MNI -38, 30, 30; 95 voxels) and right DLPFC (MNI 44, 26, 24; 106 voxels). In addition, to assess the effect of study design, a subgroup analysis was performed on 18 Tr+ experiments that only reported pre- versus post-treatment effects and revealed convergent clusters in the left (MNI -38, 30, 28; 135 voxels) and right DLPFC (MNI 44, 26, 24; 99 voxels). Following, we investigated the effect of treatment duration and performed an ALE on Tr+ effects reported after more than four weeks of treatment (12 experiments) which revealed a convergent cluster in the medial superior frontal gyrus (MNI 8, 54, 30; 104 voxels). Lastly, to assess the effect of variability in clinical outcomes, an ALE was performed on 12 Tr+ experiments which reported ≥ 50% rate of clinical response, and revealed a cluster of convergence in the left supramarginal gyrus (MNI -48, -44, 40; 123 voxels) in addition to the right DLPFC (MNI 44, 26, 24; 123 voxels).

We observed no significant convergence in the ALE meta-analysis performed on the opposite contrast among Tr- experiments (N = 21; $p_{cFWE} > 0.615$) as well as their more specific subgroups (Table 2).

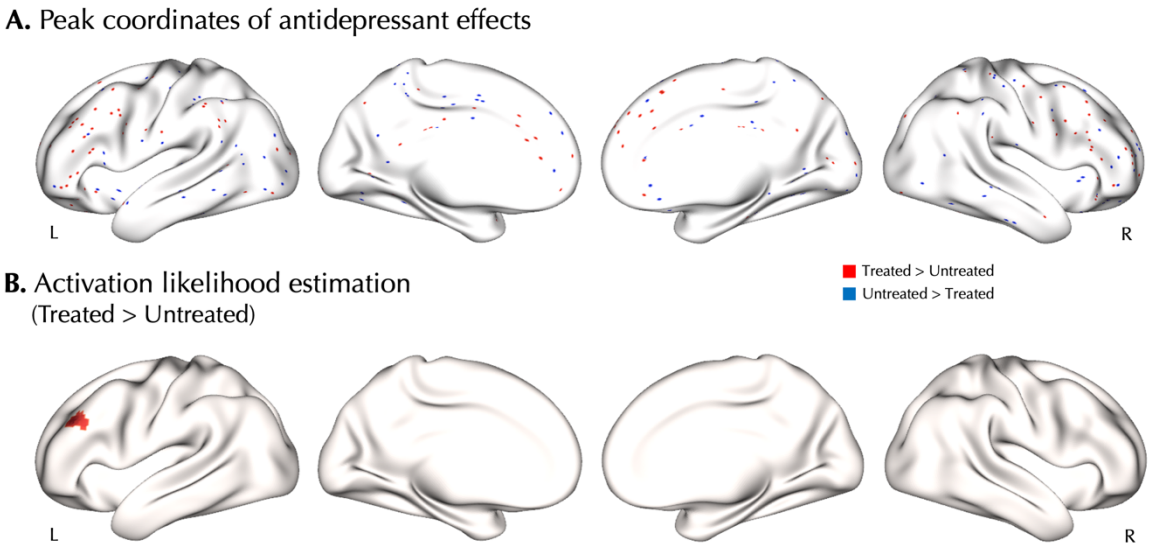

Fig. 2. Treatment-induced increase of voxel-based physiology in the left dorsolateral prefrontal cortex. A. Peak coordinates of the included experiments in Treated > Untreated (red) and Untreated > Treated (blue) comparisons. Each dot represents a peak coordinate. B. Activation

likelihood estimation showed significant convergence of Treated > Untreated comparisons in the left dorsolateral prefrontal cortex (DLPFC) after family-wise error correction at cluster level.

Functional decoding and MACM of the dorsolateral prefrontal cortex cluster

Next, we studied the behavioral relevance as well as task-based and resting-state FC of the convergent cluster identified in the main ALE meta-analysis on Tr+ experiments within the left DLPFC. Using the data from the BrainMap database, we observed that the behavioral domains of working memory (likelihood ratio = 1.85) and attention (likelihood ratio = 1.43) were significantly associated with this cluster's activation, yet they did not survive FDR correction.

The MACM of the left DLPFC cluster showed its significant co-activation with regions in the prefrontal cortex, superior parietal lobule, insula, and anterior cingulate and paracingulate cortices ($p_{cFWE} < 0.05$; Fig. 3A). The average RSFC of the left DLPFC cluster based on the HCP dataset dense connectome showed its connectivity with widespread regions in the prefrontal cortex, superior frontal gyrus, insula, anterior cingulate, paracingulate cortices, supramarginal gyrus, inferior temporal gyrus, and basal ganglia, and its anti-correlation with regions in the subgenual anterior cingulate cortex, orbitofrontal cortex, posterior cingulate, angular gyrus, and temporal pole (Fig. 3B).

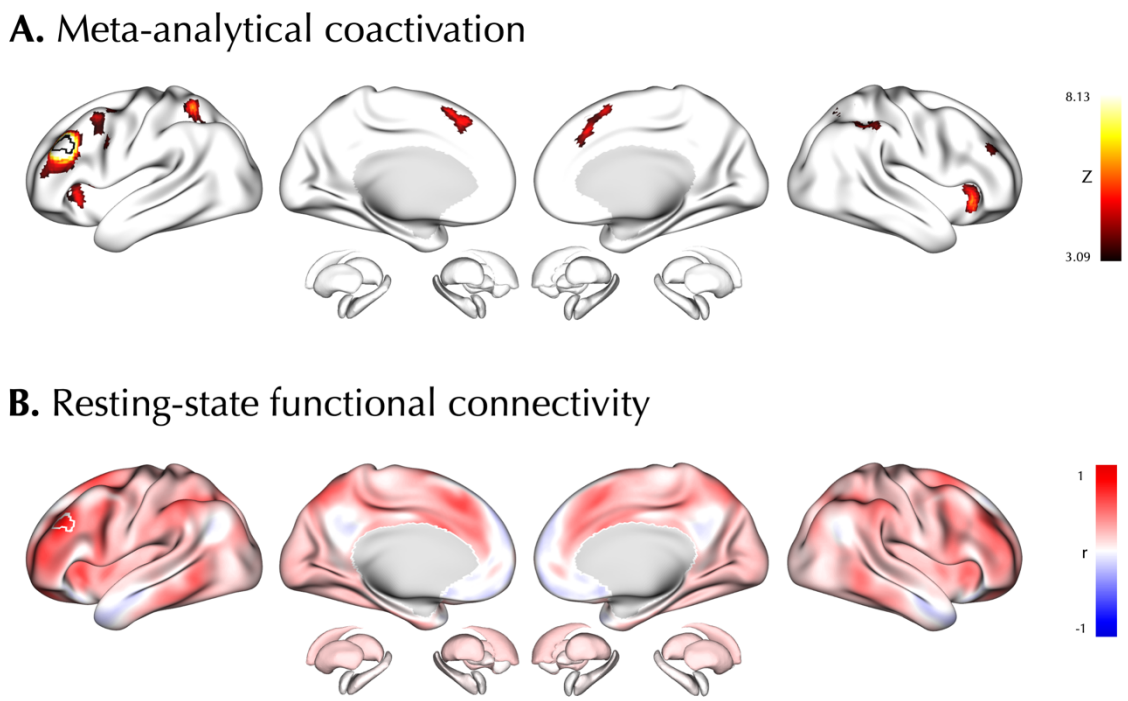

Fig. 3. Connectivity mapping of the left dorsolateral prefrontal cortex cluster. Using the center of convergent cluster at the left dorsolateral prefrontal cortex as the seed (outlined patch), the meta-analytical co-activation (A) and resting-state functional connectivity (B) maps are shown.

Convergent connectivity mapping of antidepressants' effects

MDD and its treatment are believed to affect distributed regions and networks in the brain [9], and ALE, which aims to identify *regional* convergence of localized effects cannot characterize convergence of such *distributed* effects. Therefore, we next aimed to investigate the meta-analytic effects of antidepressants at a network level, following a recently introduced approach [31]. To do so, we used the group-averaged dense functional connectome obtained from the HCP-YA dataset and quantified the convergent connectivity of the reported coordinates of antidepressant effects, which was compared against null connectivity patterns of random points.

The peak coordinates of all the included experiments, indicating alterations in functional imaging measures associated with antidepressants (512 foci from 30 experiments), showed greater-than-chance connectivity of these coordinates with widespread regions in the dorsolateral and medial prefrontal cortex, anterior insula, precuneus, supramarginal gyrus and inferior temporal gyrus. At the level of canonical resting-state networks, these foci showed significant greater-than-chance convergent connectivity to the frontoparietal (FPN; $\langle Z \rangle = 0.23$, $p_{FDR} < 0.05$) network (Fig. 4). The convergent connectivity described above was calculated by taking an average of pooled RSFC maps across experiments which was weighted by their sample sizes. Subsequently, in a sensitivity analysis we showed a similar convergent connectivity map when this weighting was not applied ($r = 0.922$, $p_{variogram} < 0.001$; Fig. S2), though at the level of canonical resting-state networks it revealed no significant effects.

The network-level analyses separately performed on the Tr+ (177 foci from 20 experiments) and Tr- effects (206 foci from 21 experiments) revealed convergent connectivity maps which were anti-correlated with each other ($r = -0.57$, $p_{variogram} < 0.001$; Fig. S3). The convergent connectivity map of all experiments (Fig. 4) was significantly correlated with the convergent connectivity map of Tr+ ($r = 0.48$, $p_{variogram} < 0.001$) but not Tr- experiments ($r = 0.051$, $p_{variogram} = 0.732$). Furthermore, the contrast-based analyses at the level of canonical resting-state networks revealed no significant greater-/lower-than-chance connectivity of the foci with these networks after FDR correction.

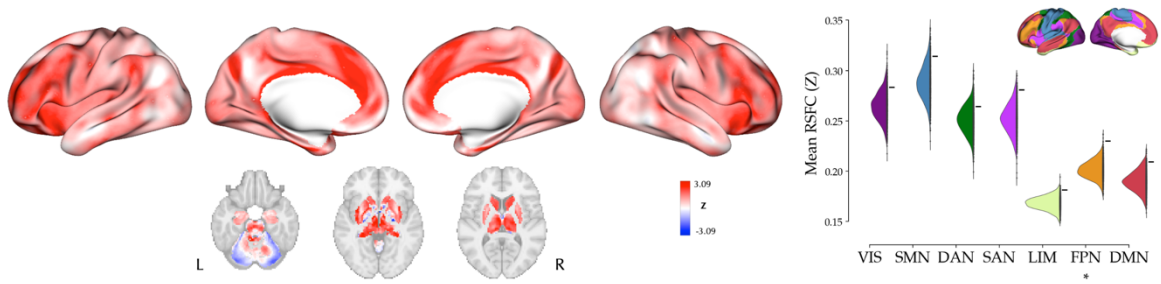

Fig. 4. Convergent connectivity mapping of antidepressant effects. *left*: The cortical and subcortical map represent Z-scored convergent connectivity map of the foci from all experiments. *right:* Mean resting-state functional connectivity (RSFC) of the observed foci across canonical resting-state networks (denoted by "-") compared against null mean values calculated based on 1000 permutations of randomly selected foci (half-violin plots). In frontoparietal network (FPN) observed mean RSFC was significantly more extreme than the null distribution in a two-tailed test.

VIS: visual network, SMN: somatomotor network, DAN: dorsal attention network, SAN: salience network, LIM: limbic network, FPN: frontoparietal network, DMN: default mode network.

The spatial localization of antidepressants' effects compared with TMS targets

The left DLPFC is one of the most common stimulation targets in the TMS treatment of MDD [99, 100]. Next, we explored whether our meta-analytic findings on the convergent effects of antidepressants might spatially correspond with the different TMS targets. We compared the location of the peak coordinate of the left DLPFC cluster identified in the Tr+ ALE meta-analysis and observed its distance with the different targets ranged from 13 to 27 mm (Fig. 5A). Moreover, the RSFC map of the Tr+ cluster showed significant correlations ($p_{variogram,\ FDR} < 0.001$), positively with the RSFC maps of "Beam F3" ($r = 0.82$) and "anti-subgenual" ($r = 0.72$) targets, but negatively with the RSFC map of "5-CM" ($r = -0.50$) target (Fig. 5B). In addition, the convergent connectivity map of antidepressant effects showed a significant and positive correlation with the RSFC of "anti-subgenual" target ($r = 0.31$, $p_{variogram,FDR} < 0.001$).

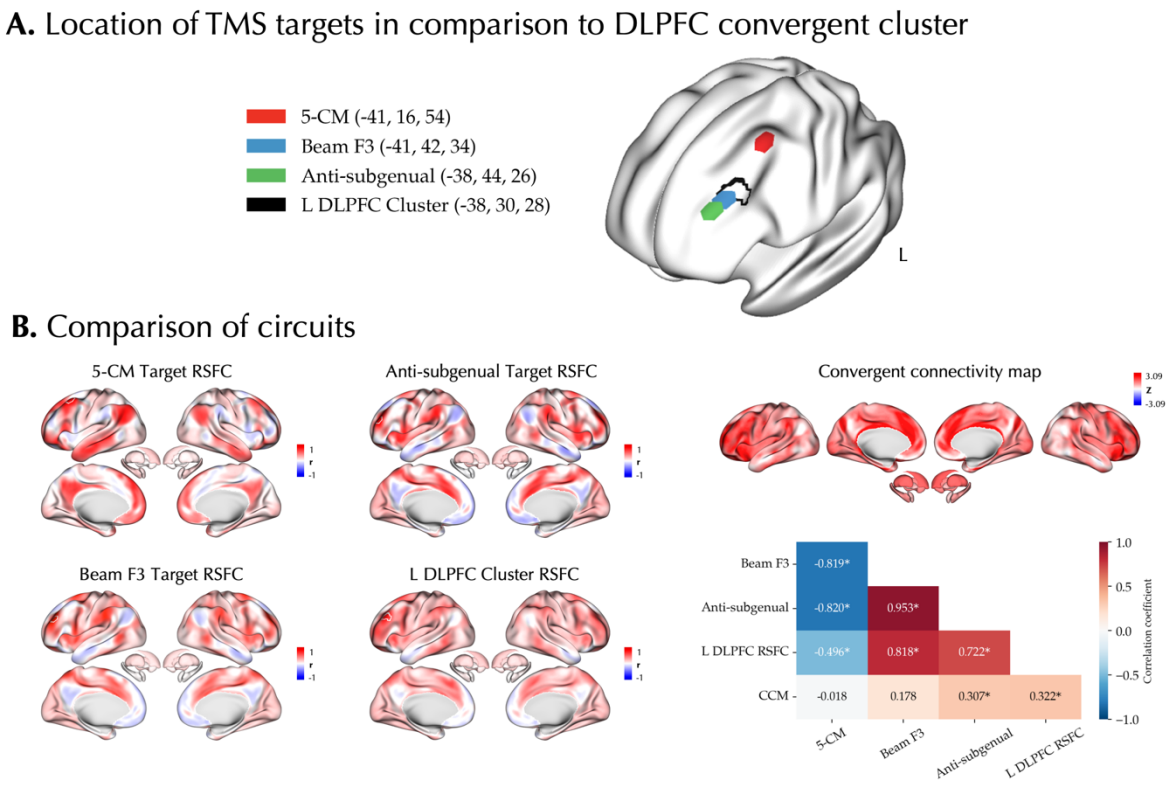

Fig 5. Association of antidepressants meta-analytic effects and transcranial magnetic stimulation targets. A. The locations of three different TMS targets is shown in comparison to the left DLPFC convergent cluster identified in the activation likelihood estimation meta-analysis on Treated > Untreated experiments. **B.** The convergent connectivity map of antidepressant effects, the RSFC map of the left DLPFC cluster, and the RSFC maps of the different TMS sites as well as their cross-correlations are shown. In the correlation matrix within each cell the Pearson correlation coefficient is reported. Asterisks denote $p_{variogram,\ FDR} < 0.05$.

The association between neurotransmitter receptor/transporter maps and meta-analytic effects of antidepressants

Lastly, we explored whether the regional and network-level convergence of antidepressant effects co-localizes with the spatial distribution of serotoninergic and noradrenergic NRTs as well as NMDA receptor (Fig. 6A) [33]. We first focused on the cluster of convergence of Tr+ effects in the left DLPFC and quantified the median density of each NRT (normalized to a range of [0-1]) in this region, showing the varying density of the NRTs. However, after FDR correction none of the NRTs were significantly over-/under-expressed in this cluster (Fig. 6B). Next, we evaluated the correlation of the parcellated convergent connectivity map with the NRT maps and observed no significant correlations after FDR correction and while accounting for the spatial autocorrelation (Fig. 6C).

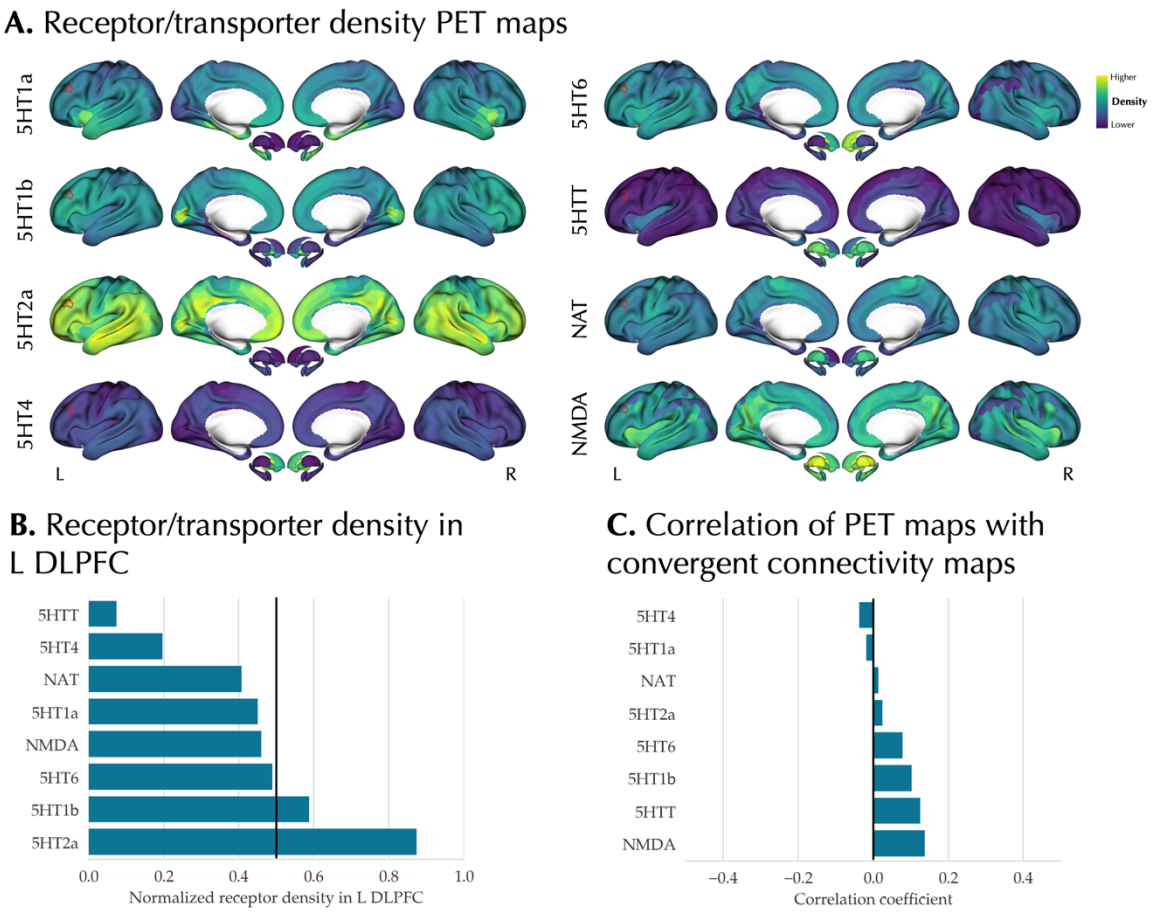

Fig. 6. Association of meta-analytic findings with neurotransmitter receptor/transporter maps. **A.** The parcellated and Z-scored PET maps of neurotransmitter receptor/transporter (NRT) are shown. Red outline indicates the left dorsolateral prefrontal cortex (L DLPFC) convergent cluster identified in the activation likelihood estimation meta-analysis on Treated > Untreated experiments. **B.** Median normalized density of NRTs in L DLPFC cluster. None of the NRTs showed significantly more extreme normalized density in this cluster compared to a null distribution created using variogram-based surrogate maps and after false discovery rate adjustment. **C.** Pearson correlation of parcellated convergent connectivity map with the NRT maps. None of the correlations were significant using variogram-based surrogates and after false discovery rate adjustment.

Discussion

In the present study, we synthesized findings of the neuroimaging literature on the brain effects associated with pharmacotherapy of MDD at regional and network levels. At the regional level, our meta-analysis showed no significant convergence across all the included experiments, though we found convergence of the reported treatment-associated increases of functional measures in the left DLPFC. This convergent cluster was associated with working memory and attention behavioral domains and showed meta-analytical connectivity with regions in the prefrontal cortex, superior parietal lobule, and insula. Extending our meta-analysis to the network level, we found greater-than-chance convergent connectivity of the reported foci of antidepressant effects primarily to the frontoparietal network. Subsequently, we found that the convergent connectivity of the foci was co-aligned with circuits connected to the "anti-subgenual" and "Beam F3" TMS targets. Last, we did not observe any significant association between the spatial pattern of the regional and network-level meta-analytic effects and the NRT maps.

Beyond regional convergence: Network-level convergent effects of antidepressants to the frontoparietal network

The pathology in MDD is increasingly thought to be distributed across brain regions and networks, rather than solely being localized [9]. Previous ALE meta-analyses aimed at identifying the *regional* convergence of abnormalities in MDD have revealed minimal or no regional convergence [32, 101, 102]. However, a recent meta-analysis by Cash *et al.* [31] revisited the functional imaging literature on brain abnormalities in MDD, aiming to identify the *network-level* convergence of abnormalities in MDD. They identified circuits of convergent connectivity related to the location of emotional and cognitive processing abnormalities in MDD, including lower-than-chance connectivity of the emotional processing abnormalities to DLPFC and pre-supplementary motor area, and greater-than-chance connectivity of the cognitive processing abnormalities to DLPFC, cingulum, insula, and precuneus [31]. Here, we found regional convergence of Tr+ functional effects in left DLPFC, yet our main ALE meta-analysis across all functional treatment effects revealed no significant regional convergence. The lack of regional convergence in our overall ALE meta-analysis, similar to the case of previous ALE meta-analyses on MDD disease effects, may be attributed to the biological and clinical heterogeneity of MDD and antidepressant effects, as well as the methodological heterogeneity of the included experiments [102]. But more importantly, it may reflect *distributed* rather than *localized* effects of antidepressants [9]. Therefore, following a similar approach to Cash et al. [31], we investigated *network-level* convergence of the reported antidepressant effects, and found their greater-than-chance connectivity in a network most prominent in the dorsolateral and medial prefrontal cortex, anterior insula, precuneus, supramarginal gyrus and inferior temporal gyrus. This circuit largely resembles the circuit of cognitive processing abnormalities in MDD [31]. Furthermore, at the level of canonical resting-state networks we found significant convergent connectivity of the reported findings with the FPN.

The convergent connectivity of reported antidepressant effects to the FPN, together with the cluster of regional convergence found in the ALE meta-analysis on the Tr+ experiments, highlights the importance of FPN and DLPFC in the therapeutic effects of antidepressants. These regions play pivotal roles in higher executive and cognitive functions of the brain,

which are shown to be impaired in patients with MDD [103–106]. Indeed, more severe executive dysfunctions are linked with higher severity of depressive symptoms [105]. The executive and cognitive dysfunction in MDD is thought to contribute to emotional dysregulation, which is a hallmark of MDD psychopathology [107, 108]. Specifically, patients with MDD might have impairments in cognitive control when processing negative emotions, deficits in the inhibition of mood-incongruent material, and difficulties in attentional disengagement from negative stimuli, which are among the mechanisms that are thought to contribute to emotional dysregulation [107, 108]. Indeed, antidepressants medications are shown to improve the executive functioning of patients with MDD, in the domains of attention and processing speed [109], psychomotor speed [110] and cognitive interference inhibition [106], and can lead to better emotional regulation strategies [111]. Hypoactivity of the prefrontal cortex in MDD is thought to contribute to the deficits of executive functioning [105, 112, 113] and emotional regulation [108, 112, 114, 115]. For instance, patients with MDD have shown a reduced activity of the DLPFC during an attentional interference task using emotional distracters [116], which can be normalized by antidepressants [117]. Furthermore, the FPN in patients with MDD shows reduced within-network connectivity and decreased connectivity with the parietal regions of the dorsal attention network, as reported by a meta-analysis on seed-based RSFC studies [118]. In addition, hypoconnectivity of the FPN with the rest of the brain has been observed in relation to depressive symptoms in the general population [119]. The treatment of MDD using various therapeutic approaches can affect intra- and inter-network connectivity of the FPN [9], DMN [120], and SAN [121–123]. Overall, MDD is characterized by altered function and connectivity of distributed networks, importantly including the FPN, but also the SAN, DMN and limbic networks, which can be modulated by the treatment (see review in Chai et al. [9]).

A similar network may be modulated by both antidepressants and TMS

The importance of DLPFC and FPN in MDD treatment has further been observed in non-pharmacological therapeutic approaches. For example, psychotherapy of patients with MDD and PTSD is shown to normalize the activity of DLPFC and increase the within-network connectivity of FPN [124]. In addition, the left DLPFC is one of the most common targets of stimulation in TMS therapy of MDD [99, 100]. High-frequency TMS applied to this region alters its activity, which in turn may have therapeutic effects by modulating the activity of its connected circuits [48, 99]. Interestingly, in our study, we found that both the convergent connectivity map of the antidepressant effects and the RSFC map of the left DLPFC cluster of convergence across Tr+ experiments were positively and significantly correlated with the "anti-subgenual" target RSFC map [50, 99, 100, 125]. Hyperactivity of the subgenual anterior cingulate cortex in MDD is thought to contribute to increased processing of negative stimuli [113]. Therefore, both the "anti-subgenual" TMS and antidepressant treatment of MDD might modulate the activity of a similar circuit, including DLPFC and sgACC. Of note, we found that the "5-CM" TMS target's circuit was anticorrelated with the circuits of "anti-subgenual" and "Beam F3" TMS targets as well as our Tr+ convergence cluster in left DLPFC. Indeed, distinct circuits connected to these different TMS targets has been previously reported, and in a retrospective study, were found to relate to clinical response in distinct clusters of depressive symptoms [125].

Lack of association between neurotranmitters and the system-level effects of antidepressants

The neurotransmitter hypothesis of MDD suggests that the dysregulation of the monoaminergic neurotransmitter systems is central to the pathophysiology of MDD, and antidepressants normalize the dysregulations of these neurotransmitter systems [5, 126, 127]. In our analyses, we found that the PET-based maps of serotoninergic and noradrenergic receptors and transporters were not significantly correlated with the regional and network-level meta-analytic effects of antidepressants. This suggests a disparity between the antidepressant effects on brain function, as observed in functional imaging studies, and the regions where their target NRTs are highly expressed. The observed divergence raises the question of what mechanisms may relate the micro-scale actions of antidepressants on the NRTs to their system-level effects on brain function. Molecular imaging techniques combined with functional imaging might provide clues to this link. The findings of molecular imaging studies in MDD and its treatment are diverse (see a comprehensive review by Ruhé et al. [127]). For example, there has been some evidence of decreased serotonin synthesis rate in the prefrontal and cingulate cortex of patients with MDD [128–130]. However, a recent umbrella review summarizing the research on the serotonin hypothesis of MDD concluded that there is a lack of convincing evidence for the association of MDD with serotoninergic deficits, such as a lower serotonin concentration or changes in the receptors [6]. Moreover, the antidepressive effects of ketamine, an NMDA receptor antagonist, highlight the importance of the other non-monoaminergic neurotransmitters in the pathophysiology and treatment of MDD [7, 8]. These findings suggest that although the monoaminergic neurotransmitter hypothesis of MDD helped us understand the pathophysiology of MDD, it may not provide a full understanding of the disease [6, 131, 132].

An overview of neuroimaging meta-analyses on MDD treatments

The neuroimaging effects of treatment in MDD have been previously investigated in a number of CBMAs [24–30]. These studies have focused on various types of treatment, with more specific (e.g., only SSRI medications [27]) or broader (e.g., pharmacotherapy, psychotherapy, and electroconvulsive therapy [29]) scopes compared to our study. In addition, various imaging modalities under different conditions have been investigated, from focusing on fMRI experiments during emotional processing tasks [30] to a broader multimodal investigation of neuroimaging experiments [29]. Given the differences in the scope and methodology of the previous CBMAs, it is not surprising that they have reported variable findings (Table 3). However, it is important to note that according to the current guidelines [21, 22], there are a few methodological issues to consider in some of the (earlier) CBMAs, which may have influenced their findings. These issues include: i) a small number of experiments included in the main or subgroup analyses, which can limit the power and increase the risk of a single experiment dominating the findings [41], ii) including explicit or hidden ROI-based experiments which are biased to inflate significance in the selected brain area, iii) using less stringent methods of multiple comparisons correction, e.g., thresholding clusters simply by applying a lenient cluster extent and height, or by using FDR, or iv) performing ALE using the earlier versions of GingerALE (< 2.3.3), in which a software bug was reported that can lead to more lenient multiple comparisons correction [133]. Here, we set out to avoid such methodological issues by

following the best-practice guidelines to conduct CBMAs [21, 22]. Furthermore, we provided network-level accounts of the effects of antidepressants reported in the literature [31], which acknowledges that the effects may be distributed rather than localized, and in doing so, complements the conventional CBMA approach of identifying regional convergence.

Future directions and limitations

In this section, we highlight areas for future research that can extend our findings and address some of our limitations. First, while our study characterizes regional and network-level convergence of antidepressant effects across multiple imaging modalities, treatments, and clinical phenotypes, more focused meta-analyses will be needed on specific selections of experiments, when more data is available in the future. Relatedly, and on the other hand, broader meta-analyses on multiple treatment modalities (including medications, psychotherapy, and brain stimulation) can extend previous work [24, 29] and address the question of whether there is a general MDD treatment effect that is shared across different therapies. Second, we studied the neuroimaging effects of antidepressant medications on patients with MDD who had received but not necessarily responded to the treatment. There is considerable variability in the clinical outcomes of antidepressant treatment [4], and this is likely to be associated with variable neuroimaging effects. To investigate the heterogeneity of imaging effects related to the clinical outcomes at the level of included studies, we performed subgroup analyses focused on experiments reporting clinical response in at least half the patients. Among the Tr+ subset of those experiments, in a small ALE, we observed convergent clusters in the left supramarginal gyrus and the right DLPFC. However, further in-depth original and meta-analytic neuroimaging studies are needed to evaluate the inter-individual variability of treatment-induced changes in brain function and its relevance to clinical response, for example, by comparing the treatment-associated functional alterations between responders and non-responders. Additionally, utilizing multivariate machine learning models on imaging, genetics, and clinical data could provide valuable insights into the inter-individual variability among MDD patients in terms of disease characteristics and in turn, response to treatment, which is critical towards personalized treatment [134–136]. Third, as we did not restrict our data to randomized controlled trials, the included subjects may have received other interventions such as psychotherapy, which may confound the results. This issue can be addressed in a future meta-analysis focused on randomized controlled trials, when more studies are available. Fourth, our network-level meta-analysis was performed using a group-averaged functional connectome based on resting-state imaging data of healthy subjects, and therefore, provides an indirect view on network-level actions of antidepressants. Further large-scale studies are needed to investigate these effects using individual-level connectomic approaches on MDD patients treated with antidepressants.

Conclusion

This comprehensive meta-analysis of the functional neuroimaging studies on the regional and network-level convergence of the effects of antidepressant medications in MDD underscores the importance of the FPN and particularly DLPFC. This observation may be attributed to the key roles of these regions in executive functions and emotional processing. The convergent regional and connectivity maps of antidepressant effects engaged circuits similar to those of "anti-subgenual" and "Beam F3" TMS targets, which may indicate common circuits are

targeted by these different treatment modalities. Lastly, we identified no associations between our regional and network-level meta-analytic findings with the spatial maps of neurotransmitter receptors/transporters, suggesting that the localized functional effects of antidepressants cannot be directly explained by the localization of these receptors/transporters. Our study highlights the need for future research integrating multiple levels of antidepressant actions at the micro- and macroscale in the context of inter-individual variability of patients with MDD and their heterogeneous clinical outcomes.

Acknowledgements

AS and SLV were funded by the Max Planck Society (Otto Hahn award) and Helmholtz Association's Initiative and Networking Fund under the Helmholtz International Lab grant agreement InterLabs-0015, and the Canada First Research Excellence Fund (CFREF Competition 2, 2015–2016) awarded to the Healthy Brains, Healthy Lives initiative at McGill University, through the Helmholtz International BigBrain Analytics and Learning Laboratory (HIBALL). SBE was supported by the Deutsche Forschungsgemeinschaft (DFG, EI 816/21-1), the National Institute of Mental Health (R01-MH074457), and the European Union's Horizon 2020 Research and Innovation Programme under Grant Agreement No. 945539 (HBP SGA3).

Conflicts of Interest

The authors declare that the research was conducted in the absence of any commercial or financial relationships that could be construed as a potential conflict of interest.

References

1. Liu Q, He H, Yang J, Feng X, Zhao F, Lyu J. Changes in the global burden of depression from 1990 to 2017: Findings from the Global Burden of Disease study. J Psychiatr Res. 2020;126:134–140.
2. Cuijpers P, Stringaris A, Wolpert M. Treatment outcomes for depression: challenges and opportunities. Lancet Psychiatry. 2020;7:925–927.
3. de Vries YA, Roest AM, Bos EH, Burgerhof JGM, van Loo HM, de Jonge P. Predicting antidepressant response by monitoring early improvement of individual symptoms of depression: individual patient data meta-analysis. Br J Psychiatry. 2019;214:4–10.
4. Undurraga J, Baldessarini RJ. Randomized, placebo-controlled trials of antidepressants for acute major depression: thirty-year meta-analytic review. Neuropsychopharmacology. 2012;37:851–864.
5. Hillhouse TM, Porter JH. A brief history of the development of antidepressant drugs: from monoamines to glutamate. Exp Clin Psychopharmacol. 2015;23:1–21.
6. Moncrieff J, Cooper RE, Stockmann T, Amendola S, Hengartner MP, Horowitz MA. The serotonin theory of depression: a systematic umbrella review of the evidence. Mol Psychiatry. 2022:1–14.
7. Coyle CM, Laws KR. The use of ketamine as an antidepressant: a systematic review and meta-analysis. Hum Psychopharmacol. 2015;30:152–163.
8. Demchenko I, Tassone VK, Kennedy SH, Dunlop K, Bhat V. Intrinsic Connectivity Networks of Glutamate-Mediated Antidepressant Response: A Neuroimaging Review. Front Psychiatry. 2022;13:864902.
9. Chai Y, Sheline YI, Oathes DJ, Balderston NL, Rao H, Yu M. Functional connectomics in depression: insights into therapies. Trends in Cognitive Sciences. 2023;27:814–832.
10. Wessa M, Lois G. Brain Functional Effects of Psychopharmacological Treatment in Major Depression: a Focus on Neural Circuitry of Affective Processing. Curr Neuropharmacol. 2015;13:466–479.
11. Bellani M, Dusi N, Yeh P-H, Soares JC, Brambilla P. The effects of antidepressants on human brain as detected by imaging studies. Focus on major depression. Prog Neuropsychopharmacol Biol Psychiatry. 2011;35:1544–1552.
12. Fu CH, Williams SC, Brammer MJ, Suckling J, Kim J, Cleare AJ, et al. Neural responses to happy facial expressions in major depression following antidepressant treatment. The American Journal of Psychiatry. 2007;164:599–607.
13. Fu CH, Williams SC, Cleare AJ, Brammer MJ, Walsh ND, Kim J, et al. Attenuation of the neural response to sad faces in major depression by antidepressant treatment: a prospective, event-related functional magnetic resonance imaging study. Archives of General Psychiatry. 2004;61:877–889.
14. Robertson B, Wang L, Diaz MT, Aiello M, Gersing K, Beyer J, et al. Effect of bupropion extended release on negative emotion processing in major depressive disorder: A pilot functional magnetic resonance imaging study. Journal of Clinical Psychiatry. 2007;68:261–267.
15. Mayberg HS, Brannan SK, Tekell JL, Silva JA, Mahurin RK, McGinnis S, et al. Regional metabolic effects of fluoxetine in major depression: Serial changes and relationship to clinical response. Biological Psychiatry. 2000;48:830–843.
16. Wang L, Li K, Zhang Q, Zeng Y, Dai W, Su Y, et al. Short-term effects of escitalopram on regional brain function in first-episode drug-naive patients with major depressive disorder assessed by resting-state functional magnetic resonance imaging. Psychological Medicine. 2014;44:1417–1426.
17. Cheng Y, Xu J, Arnone D, Nie B, Yu H, Jiang H, et al. Resting-state brain alteration after a single dose of SSRI administration predicts 8-week remission of patients with major depressive disorder. Psychological Medicine. 2017;47:438–450.
18. Wang L, Li X, Li K, Su Y, Zeng Y, Zhang Q, et al. Mapping the effect of escitalopram treatment on amplitude of low-frequency fluctuations in patients with depression: a resting-state fMRI study. Metabolic Brain Disease. 2017;32:147–154.

19. Botvinik-Nezer R, Holzmeister F, Camerer CF, Dreber A, Huber J, Johannesson M, et al. Variability in the analysis of a single neuroimaging dataset by many teams. Nature. 2020;582:84–88.
20. Poldrack RA, Baker CI, Durnez J, Gorgolewski KJ, Matthews PM, Munafò MR, et al. Scanning the horizon: towards transparent and reproducible neuroimaging research. Nat Rev Neurosci. 2017;18:115–126.
21. Müller VI, Cieslik EC, Laird AR, Fox PT, Radua J, Mataix-Cols D, et al. Ten simple rules for neuroimaging meta-analysis. Neuroscience & Biobehavioral Reviews. 2018;84:151–161.
22. Tahmasian M, Sepehry AA, Samea F, Khodadadifar T, Soltaninejad Z, Javaheripour N, et al. Practical recommendations to conduct a neuroimaging meta-analysis for neuropsychiatric disorders. Hum Brain Mapp. 2019;40:5142–5154.
23. Eickhoff SB, Bzdok D, Laird AR, Kurth F, Fox PT. Activation likelihood estimation meta-analysis revisited. Neuroimage. 2012;59:2349–2361.
24. Boccia M, Piccardi L, Guariglia P. How treatment affects the brain: meta-analysis evidence of neural substrates underpinning drug therapy and psychotherapy in major depression. Brain Imaging Behav. 2016;10:619–627.
25. Chau DT, Fogelman P, Nordanskog P, Drevets WC, Hamilton JP. Distinct Neural-Functional Effects of Treatments With Selective Serotonin Reuptake Inhibitors, Electroconvulsive Therapy, and Transcranial Magnetic Stimulation and Their Relations to Regional Brain Function in Major Depression: A Meta-analysis. Biol Psychiatry Cogn Neurosci Neuroimaging. 2017;2:318–326.
26. Delaveau P, Jabourian M, Lemogne C, Guionnet S, Bergouignan L, Fossati P. Brain effects of antidepressants in major depression: a meta-analysis of emotional processing studies. J Affect Disord. 2011;130:66–74.
27. Fitzgerald PB, Laird AR, Maller J, Daskalakis ZJ. A meta-analytic study of changes in brain activation in depression. Human Brain Mapping. 2008;29:683–695.
28. Graham J, Salimi-Khorshidi G, Hagan C, Walsh N, Goodyer I, Lennox B, et al. Meta-analytic evidence for neuroimaging models of depression: state or trait? J Affect Disord. 2013;151:423–431.
29. Li C, Hu Q, Zhang D, Hoffstaedter F, Bauer A, Elmenhorst D. Neural correlates of affective control regions induced by common therapeutic strategies in major depressive disorders: an Activation Likelihood Estimation meta-analysis study. Neuroscience & Biobehavioral Reviews. 2022:104643.
30. Ma Y. Neuropsychological mechanism underlying antidepressant effect: a systematic meta-analysis. Mol Psychiatry. 2015;20:311–319.
31. Cash RFH, Müller VI, Fitzgerald PB, Eickhoff SB, Zalesky A. Altered brain activity in unipolar depression unveiled using connectomics. Nat Mental Health. 2023;1:174–185.
32. Müller VI, Cieslik EC, Serbanescu I, Laird AR, Fox PT, Eickhoff SB. Altered Brain Activity in Unipolar Depression Revisited: Meta-analyses of Neuroimaging Studies. JAMA Psychiatry. 2017;74:47–55.
33. Hansen JY, Shafiei G, Markello RD, Smart K, Cox SML, Nørgaard M, et al. Mapping neurotransmitter systems to the structural and functional organization of the human neocortex. Nat Neurosci. 2022;25:1569–1581.
34. Page MJ, McKenzie JE, Bossuyt PM, Boutron I, Hoffmann TC, Mulrow CD, et al. The PRISMA 2020 statement: an updated guideline for reporting systematic reviews. BMJ. 2021;372:n71.
35. Fox PT, Laird AR, Fox SP, Fox PM, Uecker AM, Crank M, et al. BrainMap taxonomy of experimental design: description and evaluation. Hum Brain Mapp. 2005;25:185–198.
36. Fox PT, Lancaster JL. Opinion: Mapping context and content: the BrainMap model. Nat Rev Neurosci. 2002;3:319–321.
37. Laird AR, Lancaster JL, Fox PT. BrainMap: the social evolution of a human brain mapping database. Neuroinformatics. 2005;3:65–78.
38. Vanasse TJ, Fox PM, Barron DS, Robertson M, Eickhoff SB, Lancaster JL, et al. BrainMap VBM: An environment for structural meta-analysis. Hum Brain Mapp. 2018;39:3308–3325.

39. Lancaster JL, Tordesillas-Gutiérrez D, Martinez M, Salinas F, Evans A, Zilles K, et al. Bias between MNI and Talairach coordinates analyzed using the ICBM-152 brain template. Hum Brain Mapp. 2007;28:1194–1205.
40. Turkeltaub PE, Eickhoff SB, Laird AR, Fox M, Wiener M, Fox P. Minimizing within-experiment and within-group effects in Activation Likelihood Estimation meta-analyses. Hum Brain Mapp. 2012;33:1–13.
41. Eickhoff SB, Nichols TE, Laird AR, Hoffstaedter F, Amunts K, Fox PT, et al. Behavior, sensitivity, and power of activation likelihood estimation characterized by massive empirical simulation. Neuroimage. 2016;137:70–85.
42. Müller VI, Cieslik EC, Laird AR, Fox PT, Eickhoff SB. Dysregulated left inferior parietal activity in schizophrenia and depression: functional connectivity and characterization. Front Hum Neurosci. 2013;7:268.
43. Laird AR, Eickhoff SB, Kurth F, Fox PM, Uecker AM, Turner JA, et al. ALE Meta-Analysis Workflows Via the Brainmap Database: Progress Towards A Probabilistic Functional Brain Atlas. Front Neuroinform. 2009;3:23.
44. Glasser MF, Sotiropoulos SN, Wilson JA, Coalson TS, Fischl B, Andersson JL, et al. The minimal preprocessing pipelines for the Human Connectome Project. Neuroimage. 2013;80:105–124.
45. Van Essen DC, Smith SM, Barch DM, Behrens TEJ, Yacoub E, Ugurbil K, et al. The WU-Minn Human Connectome Project: an overview. Neuroimage. 2013;80:62–79.
46. Markello RD, Hansen JY, Liu Z-Q, Bazinet V, Shafiei G, Suárez LE, et al. neuromaps: structural and functional interpretation of brain maps. Nat Methods. 2022;19:1472–1479.
47. Yeo BTT, Krienen FM, Sepulcre J, Sabuncu MR, Lashkari D, Hollinshead M, et al. The organization of the human cerebral cortex estimated by intrinsic functional connectivity. J Neurophysiol. 2011;106:1125–1165.
48. Cash RFH, Cocchi L, Lv J, Wu Y, Fitzgerald PB, Zalesky A. Personalized connectivity-guided DLPFC-TMS for depression: Advancing computational feasibility, precision and reproducibility. Hum Brain Mapp. 2021;42:4155–4172.
49. Trapp NT, Bruss J, Johnson MK, Uitermarkt BD, Garrett L, Heinzerling A, et al. Reliability of Targeting Methods in TMS for Depression: Beam F3 vs. 5.5 cm. Brain Stimul. 2020;13:578–581.
50. Blumberger DM, Vila-Rodriguez F, Thorpe KE, Feffer K, Noda Y, Giacobbe P, et al. Effectiveness of theta burst versus high-frequency repetitive transcranial magnetic stimulation in patients with depression (THREE-D): a randomised non-inferiority trial. The Lancet. 2018;391:1683–1692.
51. Burt JB, Helmer M, Shinn M, Anticevic A, Murray JD. Generative modeling of brain maps with spatial autocorrelation. NeuroImage. 2020;220:117038.
52. Baldassarri SR, Park E, Finnema SJ, Planeta B, Nabulsi N, Najafzadeh S, et al. Inverse changes in raphe and cortical 5-HT1B receptor availability after acute tryptophan depletion in healthy human subjects. Synapse. 2020;74:e22159.
53. Belfort-DeAguiar R, Gallezot J-D, Hwang JJ, Elshafie A, Yeckel CW, Chan O, et al. Noradrenergic Activity in the Human Brain: A Mechanism Supporting the Defense Against Hypoglycemia. J Clin Endocrinol Metab. 2018;103:2244–2252.
54. Beliveau V, Ganz M, Feng L, Ozenne B, Højgaard L, Fisher PM, et al. A High-Resolution In Vivo Atlas of the Human Brain's Serotonin System. J Neurosci. 2017;37:120–128.
55. Ding Y-S, Singhal T, Planeta-Wilson B, Gallezot J-D, Nabulsi N, Labaree D, et al. PET Imaging of the Effects of Age and Cocaine on the Norepinephrine Transporter in the Human Brain Using (S,S)-[11C]O-Methylreboxetine and HRRT. Synapse. 2010;64:30–38.
56. Gallezot J-D, Nabulsi N, Neumeister A, Planeta-Wilson B, Williams WA, Singhal T, et al. Kinetic modeling of the serotonin 5-HT1B receptor radioligand [11C]P943 in humans. J Cereb Blood Flow Metab. 2010;30:196–210.
57. Galovic M, Al-Diwani A, Vivekananda U, Torrealdea F, Erlandsson K, Fryer TD, et al. In vivo NMDA receptor function in people with NMDA receptor antibody encephalitis. 2021:2021.12.04.21267226.

58. Galovic M, Erlandsson K, Fryer TD, Hong YT, Manavaki R, Sari H, et al. Validation of a combined image derived input function and venous sampling approach for the quantification of [18F]GE-179 PET binding in the brain. Neuroimage. 2021;237:118194.
59. Li CR, Potenza MN, Lee DE, Planeta B, Gallezot J-D, Labaree D, et al. Decreased norepinephrine transporter availability in obesity: Positron Emission Tomography imaging with (S,S)-[(11)C]O-methylreboxetine. Neuroimage. 2014;86:306–310.
60. Matuskey D, Bhagwagar Z, Planeta B, Pittman B, Gallezot J-D, Chen J, et al. Reductions in Brain 5-HT1B Receptor Availability in Primarily Cocaine-Dependent Humans. Biol Psychiatry. 2014;76:816–822.
61. McGinnity CJ, Hammers A, Riaño Barros DA, Luthra SK, Jones PA, Trigg W, et al. Initial evaluation of 18F-GE-179, a putative PET Tracer for activated N-methyl D-aspartate receptors. J Nucl Med. 2014;55:423–430.
62. Murrough JW, Czermak C, Henry S, Nabulsi N, Gallezot J-D, Gueorguieva R, et al. The effect of early trauma exposure on serotonin type 1B receptor expression revealed by reduced selective radioligand binding. Arch Gen Psychiatry. 2011;68:892–900.
63. Murrough JW, Henry S, Hu J, Gallezot J-D, Planeta-Wilson B, Neumaier JF, et al. Reduced ventral striatal/ventral pallidal serotonin1B receptor binding potential in major depressive disorder. Psychopharmacology (Berl). 2011;213:547–553.
64. Pittenger C, Adams TG, Gallezot J-D, Crowley MJ, Nabulsi N, James Ropchan null, et al. OCD is associated with an altered association between sensorimotor gating and cortical and subcortical 5-HT1b receptor binding. J Affect Disord. 2016;196:87–96.
65. Radhakrishnan R, Matuskey D, Nabulsi N, Gaiser E, Gallezot J-D, Henry S, et al. In vivo 5-HT6 and 5-HT2A receptor availability in antipsychotic treated schizophrenia patients vs. unmedicated healthy humans measured with [11C]GSK215083 PET. Psychiatry Res Neuroimaging. 2020;295:111007.
66. Radhakrishnan R, Nabulsi N, Gaiser E, Gallezot J-D, Henry S, Planeta B, et al. Age-Related Change in 5-HT6 Receptor Availability in Healthy Male Volunteers Measured with 11C-GSK215083 PET. J Nucl Med. 2018;59:1445–1450.
67. Sanchez-Rangel E, Gallezot J-D, Yeckel CW, Lam W, Belfort-DeAguiar R, Chen M-K, et al. Norepinephrine transporter availability in brown fat is reduced in obesity: a human PET study with [11C] MRB. Int J Obes (Lond). 2020;44:964–967.
68. Saricicek A, Chen J, Planeta B, Ruf B, Subramanyam K, Maloney K, et al. Test-retest reliability of the novel 5-HT1B receptor PET radioligand [11C]P943. Eur J Nucl Med Mol Imaging. 2015;42:468–477.
69. Savli M, Bauer A, Mitterhauser M, Ding Y-S, Hahn A, Kroll T, et al. Normative database of the serotonergic system in healthy subjects using multi-tracer PET. NeuroImage. 2012;63:447–459.
70. Abdallah CG, Averill LA, Collins KA, Geha P, Schwartz J, Averill C, et al. Ketamine Treatment and Global Brain Connectivity in Major Depression. Neuropsychopharmacology : Official Publication of the American College of Neuropsychopharmacology. 2017;42:1210–1219.
71. Bremner JD, Vythilingam M, Vermetten E, Charney DS. Effects of antidepressant treatment on neural correlates of emotional and neutral declarative verbal memory in depression. J Affect Disord. 2007;101:99–111.
72. Carlson PJ, Diazgranados N, Nugent AC, Ibrahim L, Luckenbaugh DA, Brutsche N, et al. Neural correlates of rapid antidepressant response to ketamine in treatment-resistant unipolar depression: a preliminary positron emission tomography study. Biological Psychiatry. 2013;73:1213–1221.
73. Downey D, Dutta A, McKie S, Dawson GR, Dourish CT, Craig K, et al. Comparing the actions of lanicemine and ketamine in depression: key role of the anterior cingulate. Eur Neuropsychopharmacol. 2016;26:994–1003.
74. Fonzo GA, Etkin A, Zhang Y, Wu W, Cooper C, Chin-Fatt C, et al. Brain regulation of emotional conflict predicts antidepressant treatment response for depression. Nature Human Behaviour. 2019;3:1319–1331.
75. Frodl T, Scheuerecker J, Schoepf V, Linn J, Koutsouleris N, Bokde ALW, et al. Different effects of mirtazapine and venlafaxine on brain activation: An open randomized controlled fMRI study. Journal of Clinical Psychiatry. 2011;72:448–457.

76. Fu CHY, Costafreda SG, Sankar A, Adams TM, Rasenick MM, Liu P, et al. Multimodal functional and structural neuroimaging investigation of major depressive disorder following treatment with duloxetine. BMC Psychiatry. 2015;15:82.
77. Gonzalez S, Vasavada MM, Njau S, Sahib AK, Espinoza R, Narr KL, et al. Acute changes in cerebral blood flow after single-infusion ketamine in major depression: A pilot study. Neurology Psychiatry and Brain Research. 2020;38:5–11.
78. Jiang W, Yin Z, Pang Y, Wu F, Kong L, Xu K. Brain functional changes in facial expression recognition in patients with major depressive disorder before and after antidepressant treatment: A functional magnetic resonance imaging study. Neural Regeneration Research. 2012;7:1151–1157.
79. Joe AY, Tielmann T, Bucerius J, Reinhardt MJ, Palmedo H, Maier W, et al. Response-Dependent Differences in Regional Cerebral Blood Flow Changes with Citalopram in Treatment of Major Depression. Journal of Nuclear Medicine. 2006;47:1319–1325.
80. Keedwell P, Drapier D, Surguladze S, Giampietro V, Brammer M, Phillips M. Neural markers of symptomatic improvement during antidepressant therapy in severe depression: subgenual cingulate and visual cortical responses to sad, but not happy, facial stimuli are correlated with changes in symptom score. J Psychopharmacol. 2009;23:775–788.
81. Kennedy SH, Evans KR, Kruger S, Mayberg HS, Meyer JH, McCann S, et al. Changes in regional brain glucose metabolism measured with positron emission tomography after paroxetine treatment of major depression. American Journal of Psychiatry. 2001;158:899–905.
82. Kohn Y, Freedman N, Lester H, Krausz Y, Chisin R, Lerer B, et al. Cerebral perfusion after a 2-year remission in major depression. International Journal of Neuropsychopharmacology. 2008;11:837–843.
83. Komulainen E, Heikkila R, Nummenmaa L, Raij TT, Harmer CJ, Isometsa E, et al. Short-term escitalopram treatment normalizes aberrant self-referential processing in major depressive disorder. Journal of Affective Disorders. 2018;236:222–229.
84. Komulainen E, Glerean E, Heikkilä R, Nummenmaa L, Raij TT, Isometsä E, et al. Escitalopram enhances synchrony of brain responses during emotional narratives in patients with major depressive disorder. Neuroimage. 2021;237:118110.
85. Kraus C, Klöbl M, Tik M, Auer B, Vanicek T, Geissberger N, et al. The pulvinar nucleus and antidepressant treatment: dynamic modeling of antidepressant response and remission with ultra-high field functional MRI. Mol Psychiatry. 2019;24:746–756.
86. Li CT, Chen MH, Lin WC, Hong CJ, Yang BH, Liu RS, et al. The effects of low-dose ketamine on the prefrontal cortex and amygdala in treatment-resistant depression: A randomized controlled study. Human Brain Mapping. 2016;37:1080–1090.
87. Lopez-Sola M, Pujol J, Hernandez-Ribas R, Harrison BJ, Contreras-Rodriguez O, Soriano-Mas C, et al. Effects of Duloxetine Treatment on Brain Response to Painful Stimulation in Major Depressive Disorder. Neuropsychopharmacology. 2010;35:2305–2317.
88. Murrough JW, Collins KA, Fields J, DeWilde KE, Phillips ML, Mathew SJ, et al. Regulation of neural responses to emotion perception by ketamine in individuals with treatment-resistant major depressive disorder. Translational Psychiatry. 2015;5.
89. Reed JL, Nugent AC, Furey ML, Szczepanik JE, Evans JW, Zarate CA. Ketamine normalizes brain activity during emotionally valenced attentional processing in depression. NeuroImage: Clinical. 2018;20:92–101.
90. Reed JL, Nugent AC, Furey ML, Szczepanik JE, Evans JW, Zarate CA. Effects of Ketamine on Brain Activity During Emotional Processing: Differential Findings in Depressed Versus Healthy Control Participants. Biological Psychiatry: Cognitive Neuroscience and Neuroimaging. 2019;4:610–618.
91. Rutgen M, Pletti C, Tik M, Kraus C, Pfabigan DM, Sladky R, et al. Antidepressant treatment, not depression, leads to reductions in behavioral and neural responses to pain empathy. Translational Psychiatry. 2019;9.
92. Sankar A, Adams TM, Costafreda SG, Marangell LB, Fu CH. Effects of antidepressant therapy on neural components of verbal working memory in depression. Journal of Psychopharmacology (Oxford, England). 2017;31:1176–1183.

93. Sterpenich V, Vidal S, Hofmeister J, Michalopoulos G, Bancila V, Warrot D, et al. Increased Reactivity of the Mesolimbic Reward System after Ketamine Injection in Patients with Treatment-resistant Major Depressive Disorder. Anesthesiology. 2019;130:923–935.
94. Wagner G, Koch K, Schachtzabel C, Sobanski T, Reichenbach JR, Sauer H, et al. Differential effects of serotonergic and noradrenergic antidepressants on brain activity during a cognitive control task and neurofunctional prediction of treatment outcome in patients with depression. Journal of Psychiatry and Neuroscience. 2010;35:247–257.
95. Walsh ND, Williams SC, Brammer MJ, Bullmore ET, Kim J, Suckling J, et al. A longitudinal functional magnetic resonance imaging study of verbal working memory in depression after antidepressant therapy. Biological Psychiatry. 2007;62:1236–1243.
96. Wang Y, Xu C, Cao X, Gao Q, Li J, Liu Z, et al. Effects of an antidepressant on neural correlates of emotional processing in patients with major depression. Neuroscience Letters. 2012;527:55–59.
97. Williams RJ, Brown EC, Clark DL, Pike GB, Ramasubbu R. Early post-treatment blood oxygenation level-dependent responses to emotion processing associated with clinical response to pharmacological treatment in major depressive disorder. Brain Behav. 2021;11:e2287.
98. Yin Y, Wang M, Wang Z, Xie C, Zhang H, Zhang H, et al. Decreased cerebral blood flow in the primary motor cortex in major depressive disorder with psychomotor retardation. Prog Neuropsychopharmacol Biol Psychiatry. 2018;81:438–444.
99. Fox MD, Buckner RL, White MP, Greicius MD, Pascual-Leone A. Efficacy of Transcranial Magnetic Stimulation Targets for Depression Is Related to Intrinsic Functional Connectivity with the Subgenual Cingulate. Biological Psychiatry. 2012;72:595–603.
100. O'Reardon JP, Solvason HB, Janicak PG, Sampson S, Isenberg KE, Nahas Z, et al. Efficacy and Safety of Transcranial Magnetic Stimulation in the Acute Treatment of Major Depression: A Multisite Randomized Controlled Trial. Biological Psychiatry. 2007;62:1208–1216.
101. Gray JP, Müller VI, Eickhoff SB, Fox PT. Multimodal Abnormalities of Brain Structure and Function in Major Depressive Disorder: A Meta-Analysis of Neuroimaging Studies. Am J Psychiatry. 2020;177:422–434.
102. Saberi A, Mohammadi E, Zarei M, Eickhoff SB, Tahmasian M. Structural and functional neuroimaging of late-life depression: a coordinate-based meta-analysis. Brain Imaging and Behavior. 2021. 31 July 2021. https://doi.org/10.1007/s11682-021-00494-9.
103. Lee RSC, Hermens DF, Porter MA, Redoblado-Hodge MA. A meta-analysis of cognitive deficits in first-episode Major Depressive Disorder. Journal of Affective Disorders. 2012;140:113–124.
104. Rock PL, Roiser JP, Riedel WJ, Blackwell AD. Cognitive impairment in depression: a systematic review and meta-analysis. Psychological Medicine. 2014;44:2029–2040.
105. Snyder HR. Major depressive disorder is associated with broad impairments on neuropsychological measures of executive function: a meta-analysis and review. Psychol Bull. 2013;139:81–132.
106. Wagner S, Doering B, Helmreich I, Lieb K, Tadić A. A meta-analysis of executive dysfunctions in unipolar major depressive disorder without psychotic symptoms and their changes during antidepressant treatment. Acta Psychiatr Scand. 2012;125:281–292.
107. Gotlib IH, Joormann J. Cognition and depression: current status and future directions. Annu Rev Clin Psychol. 2010;6:285–312.
108. Joormann J, Stanton CH. Examining emotion regulation in depression: A review and future directions. Behaviour Research and Therapy. 2016;86:35–49.
109. Gudayol-Ferré E, Duarte-Rosas P, Peró-Cebollero M, Guàrdia-Olmos J. The effect of second-generation antidepressant treatment on the attention and mental processing speed of patients with major depressive disorder: A meta-analysis study with structural equation models. Psychiatry Res. 2022;314:114662.
110. Rosenblat JD, Kakar R, McIntyre RS. The Cognitive Effects of Antidepressants in Major Depressive Disorder: A Systematic Review and Meta-Analysis of Randomized Clinical Trials. Int J Neuropsychopharmacol. 2015;19:pyv082.

111. McRae K, Rekshan W, Williams LM, Cooper N, Gross JJ. Effects of antidepressant medication on emotion regulation in depressed patients: an iSPOT-D report. J Affect Disord. 2014;159:127–132.
112. Davidson RJ, Pizzagalli D, Nitschke JB, Putnam K. Depression: perspectives from affective neuroscience. Annu Rev Psychol. 2002;53:545–574.
113. Disner SG, Beevers CG, Haigh EAP, Beck AT. Neural mechanisms of the cognitive model of depression. Nat Rev Neurosci. 2011;12:467–477.
114. Salehinejad MA, Ghanavai E, Rostami R, Nejati V. Cognitive control dysfunction in emotion dysregulation and psychopathology of major depression (MD): Evidence from transcranial brain stimulation of the dorsolateral prefrontal cortex (DLPFC). J Affect Disord. 2017;210:241–248.
115. Ebneabbasi A, Mahdipour M, Nejati V, Li M, Liebe T, Colic L, et al. Emotion processing and regulation in major depressive disorder: A 7T resting-state fMRI study. Hum Brain Mapp. 2021;42:797–810.
116. Fales CL, Barch DM, Rundle MM, Mintun MA, Snyder AZ, Cohen JD, et al. Altered Emotional Interference Processing in Affective and Cognitive-Control Brain Circuitry in Major Depression. Biological Psychiatry. 2008;63:377–384.
117. Fales CL, Barch DM, Rundle MM, Mintun MA, Mathews J, Snyder AZ, et al. Antidepressant treatment normalizes hypoactivity in dorsolateral prefrontal cortex during emotional interference processing in major depression. Journal of Affective Disorders. 2009;112:206–211.
118. Kaiser RH, Andrews-Hanna JR, Wager TD, Pizzagalli DA. Large-Scale Network Dysfunction in Major Depressive Disorder: A Meta-analysis of Resting-State Functional Connectivity. JAMA Psychiatry. 2015;72:603–611.
119. Schultz DH, Ito T, Solomyak LI, Chen RH, Mill RD, Anticevic A, et al. Global connectivity of the fronto-parietal cognitive control network is related to depression symptoms in the general population. Network Neuroscience. 2018;3:107–123.
120. Daws RE, Timmermann C, Giribaldi B, Sexton JD, Wall MB, Erritzoe D, et al. Increased global integration in the brain after psilocybin therapy for depression. Nat Med. 2022;28:844–851.
121. Fischer AS, Holt-Gosselin B, Fleming SL, Hack LM, Ball TM, Schatzberg AF, et al. Intrinsic reward circuit connectivity profiles underlying symptom and quality of life outcomes following antidepressant medication: a report from the iSPOT-D trial. Neuropsychopharmacol. 2021;46:809–819.
122. Liu J, Fan Y, Ling-Li Zeng, Liu B, Ju Y, Wang M, et al. The neuroprogressive nature of major depressive disorder: evidence from an intrinsic connectome analysis. Transl Psychiatry. 2021;11:1–11.
123. Mkrtchian A, Evans JW, Kraus C, Yuan P, Kadriu B, Nugent AC, et al. Ketamine modulates fronto-striatal circuitry in depressed and healthy individuals. Mol Psychiatry. 2021;26:3292–3301.
124. Yang Z, Oathes DJ, Linn KA, Bruce SE, Satterthwaite TD, Cook PA, et al. Cognitive Behavioral Therapy Is Associated With Enhanced Cognitive Control Network Activity in Major Depression and Posttraumatic Stress Disorder. Biol Psychiatry Cogn Neurosci Neuroimaging. 2018;3:311–319.
125. Siddiqi SH, Taylor SF, Cooke D, Pascual-Leone A, George MS, Fox MD. Distinct Symptom-Specific Treatment Targets for Circuit-Based Neuromodulation. American Journal of Psychiatry. 2020:appi.ajp.2019.19090915.
126. Hirschfeld RM. History and evolution of the monoamine hypothesis of depression. J Clin Psychiatry. 2000;61 Suppl 6:4–6.
127. Ruhé HG, Frokjaer VG, Haarman B (Benno) CM, Jacobs GE, Booij J. Molecular Imaging of Depressive Disorders. In: Dierckx RAJO, Otte A, de Vries EFJ, van Waarde A, Sommer IE, editors. PET and SPECT in Psychiatry, Cham: Springer International Publishing; 2021. p. 85–207.
128. Rosa-Neto P, Diksic M, Okazawa H, Leyton M, Ghadirian N, Mzengeza S, et al. Measurement of brain regional alpha-[11C]methyl-L-tryptophan trapping as a measure of serotonin synthesis in medication-free patients with major depression. Arch Gen Psychiatry. 2004;61:556–563.

129. Agren H, Reibring L. PET studies of presynaptic monoamine metabolism in depressed patients and healthy volunteers. Pharmacopsychiatry. 1994;27:2–6.
130. Agren H, Reibring L, Hartvig P, Tedroff J, Bjurling P, Hörnfeldt K, et al. Low brain uptake of L-[11C]5-hydroxytryptophan in major depression: a positron emission tomography study on patients and healthy volunteers. Acta Psychiatr Scand. 1991;83:449–455.
131. Hindmarch I. Beyond the monoamine hypothesis: mechanisms, molecules and methods. Eur Psychiatry. 2002;17 Suppl 3:294–299.
132. Taylor C, Fricker AD, Devi LA, Gomes I. Mechanisms of action of antidepressants: from neurotransmitter systems to signaling pathways. Cell Signal. 2005;17:549–557.
133. Eickhoff SB, Laird AR, Fox PM, Lancaster JL, Fox PT. Implementation errors in the GingerALE Software: Description and recommendations. Hum Brain Mapp. 2017;38:7–11.
134. Winter NR, Blanke J, Leenings R, Ernsting J, Fisch L, Sarink K, et al. A Systematic Evaluation of Machine Learning-Based Biomarkers for Major Depressive Disorder. JAMA Psychiatry. 2024;81:386–395.
135. Olfati M, Samea F, Faghihroohi S, Balajoo SM, Küppers V, Genon S, et al. Prediction of depressive symptoms severity based on sleep quality, anxiety, and brain: a machine learning approach across three cohorts. 2024:2023.08.09.23293887.
136. Cohen SE, Zantvoord JB, Wezenberg BN, Bockting CLH, van Wingen GA. Magnetic resonance imaging for individual prediction of treatment response in major depressive disorder: a systematic review and meta-analysis. Transl Psychiatry. 2021;11:1–10.

Table 1. Characteristics of studies included in this meta-analysis

#	First Author, Year [a]	N (female %) Treated / Untreated	Responded %	Age Treated / Untreated	Wash out period	Antidepressant medication	Duration between Scans	Modality
1	Abdallah, C. G., 2017	18 (44%)	55.5%	43	1 w	Ketamine	1 d	rs-fMRI (GBC)
	Murrough, J. W., 2015							tb-fMRI
2	Bremner, J. D., 2007	13 (84%)	100%	40.0[c]	4 w	Fluoxetine or Venlafaxine	6 +/- 3 m	H_2O-PET
3	Carlson, P. J., 2013	20 (30%)	30.0%	48	2 w	Ketamine	1-3 d	FDG-PET
4	Cheng, Y., 2017	38 (70%[c])	60%	28[c]	Drug-naive	Escitalopram	5 h, 4 w, 8 w	rs-fMRI (fALFF)
5	Downey, D., 2016	21 (62%) / 19 (58%)	n.a.	27.1 / 25.7	n.a.	Ketamine	45 min	rs-fMRI
6	Fonzo, G. A., 2019	96 (72%) / 105 (64%)	n.a.	37 / 36	n.a.	Sertraline	8 w	tb-fMRI
7	Frodl, T., 2011	24 (33%)	n.a.	39	1 y	Venlafaxine or Mirtazapine	4 w	tb-fMRI
8	Fu, C. H., 2004, 2007	19 (68%)	n.a.	43	n.a.	Fluoxetine	8 w	tb-fMRI
9	Fu, C. H., 2015	24 (41%[c])	79%	40.2	4 weeks	Duloxetine	12 w	tb-fMRI
10	Gonzalez, S., 2020	11 (27%)	45.4%	48	None	Ketamine	1 h, 6 h, 24 h	ASL-fMRI
11	Jiang, W., 2012	21 (57%)	100%	29	Drug-naive	Escitalopram	8-12 w	tb-fMRI
12	Joe, A.Y., 2006	35 (72%)	53.8%	45.3	n.a.	Citalopram	3 w	^{99m}Tc-HMPAO SPECT
13	Keedwell, P., 2008	12 (50%)	66%	49.0	Drug-naive	Variable	6 – 18 w	tb-fMRI
14	Kennedy, S. H., 2001	13 (0%)	100%	37	4 w	Paroxetine	6 w	FDG-PET

15	Kohn, Y., 2008	11 (54%)	100%	49	Variable	Paroxetine, Fluoxetine or Clomipramine	2 y	^{99m}Tc-HMPAO SPECT
16	Komulainen, E., 2018	17 (53%) / 15 (60%)	n.a.	27 / 23	4 m	Escitalopram	1 w	tb-fMRI
	Komulainen, E., 2021	15 (53%) / 14 (57%)	n.a.	29 / 24	n.a.			
17	Kraus, C., 2019	26 (73%) / 36 (63%)	84%	30.4 / 28.5	3 m	Escitalopram ± Venlafaxine or Mitrazapine	12 w	tb-fMRI
	Rütgen, M., 2019	29 (72%)	75.8%	30	3 m			
18	Li, C. T., 2016	32 (69%)	31.2%	44	n.a.	Ketamine	1 h	FDG-PET
19	Lopez-Sola, M., 2010	13 (85%)	69.2%	45	15 d	Duloxetine	1 w, 8 w	tb-fMRI
20	Mayberg, H. S., 2000	10 (0%)	50.0%	49[c]	1 m	Fluoxetine	1 w, 6 w	FDG-PET
21	Reed, J. L., 2018, 2019	28 (64%[c])	n.a.	36[c]	2 w	Ketamine	2d, 11d	tb-fMRI
22	Robertson, B., 2007	8 (75%)	75%	41[c]	n.a.	Bupropion	8 w	tb-fMRI
23	Sankar, A., 2017	23 (56%)	78.2%	40	4 w	Duloxetine	12 w	tb-fMRI
24	Sterpenich, V., 2019	10 (60%)	n.a.	51	None	Ketamine	1 d, 7 d	tb-fMRI
25	Wagner, G., 2010	20 (90%)	50.0%	39	Variable	Citalopram or Reboxetine	6 w	tb-fMRI
26	Walsh, N. D., 2007	20 (70%)	75.0%	44	n.a.	Fluoxetine	8 w	tb-fMRI
27	Wang, L., 2014	14 (36%)	100%	33	Drug-naive	Escitalopram	8 w	rs-fMRI (ReHo)
	Wang, L., 2017	20 (55%)	100%	35				rs-fMRI (fALFF)
28	Wang, Y., 2012	18 (61%)	n.a.	32	Drug-naive	Fluoxetine	8 w	tb-fMRI
29	Williams, R. J., 2021	38 (68%)	57% (after 8 weeks)	36.2	n.a.	Citalopram or Quetiapine	1 w	tb-fMRI
30	Yin, Y., 2018	11 (36%)	100%	49.2	4 w	Variable	8 w	ASL-fMRI

[a] Publications with overlapping samples are grouped together, [b] Mean or median, [c] Reported for all the subjects rather than those in the included experiment

n.a.: not available, fMRI: functional magnetic resonance imaging, rs-fMRI: resting-state fMRI, tb-fMRI: task based fMRI, ASL-fMRI: arterial spin labeling fMRI, FDG-PET: fluorodeoxyglucose-positron emission tomography, SPECT: single-photon emission computed tomography, GBC: global brain connectivity, fALFF: fractional amplitude of low-frequency fluctuations, ReHo: regional homogeneity, ASL: arterial spin labeling.

Table 2. Activation Likelihood Estimation (ALE) analyses on the effects of antidepressants in major depressive disorder

Experiments	Comparison	N	Min p_{cFWE}[a]	Convergence
All	All	30	0.387	-
	Treated > Untreated	20	**0.005**	L DLPFC
	Treated < Untreated	21	0.615	-
Based on modality				
Rest	All	12	0.052	-
Task	All	19	0.970	-
Based on treatment and clinical setting				
Excluding ketamine	All	23	0.486	-
	Treated > Untreated	14	**0.024**	L DLPFC, R DLPFC
	Treated < Untreated	16	0.464	-
Pre- versus post-treatment effects	All	24	0.294	-
	Treated > Untreated	18	**0.004**	L DLPFC, R DLPFC
	Treated < Untreated	20	0.469	-
Treatment duration > 4 weeks	All	20	0.472	-
	Treated > Untreated	12	**0.010**	R mSFG
	Treated < Untreated	14	0.189	-
Response in ≥50% of subjects	All	19	0.614	-
	Treated > Untreated	12	**0.007**	L SMG, R DLPFC
	Treated < Untreated	15	0.357	-

[a] Bold p-values indicate statistical significance.

cFWE: cluster-wise family-wise error, SSRI: selective serotonin reuptake inhibitor, L: left, R: right, DLPFC: dorsolateral prefrontal cortex, mSFG: medial superior frontal gyrus, SMG: supramarginal gyrus.

Table 3. Comparison of the existing coordinate-based neuroimaging meta-analyses on the brain effects of antidepressants.

CBMA	N studies[a]	Treatment	Imaging	Method	Findings
Fitzgerald et al., 2008	9	SSRI	PET, SPECT (resting-state)	ALE, FDR-corrected, BrainMap	↑: middle frontal gyrus, inferior frontal gyrus, anterior cingulate cortex, precentral gyrus, supramarginal gyrus, posterior cingulate gyrus, inferior parietal lobe, midbrain, putamen ↓: middle and superior frontal gyri, medial frontal gyrus, subgenual and pregenual anterior cingulate, parahippocampal gyrus, hippocampus, insula, putamen
Delaveau et al., 2011	9	Antidepressants	fMRI, PET (emotional activation)	ALE, FDR-corrected, GingerALE 2.0	↑: dorsal medial prefrontal cortex, dorsolateral prefrontal cortex, cuneus, fusiform gyrus, lingual gyrus, middle temporal gyrus, putamen, caudate, thalamus, anterior insula, anterior cingulate cortex ↓: thalamus, caudate, putamen, globus pallidus, hippocampus, amygdala, parahippocampal gyrus, anterior insula, anterior cingulate cortex, orbitofrontal cortex, posterior cingulate cortex, middle frontal gyrus, pre/postcentral gyri, lingual gyrus, cerebellum, supramarginal gyrus, fusiform gyrus
Graham et al., 2013	4	Any	fMRI	ALE / GPR, FDR-corrected, GingerALE 2.1 / custom code	↑: - (ALE), precentral gyrus, precuneus, dorsolateral prefrontal cortex (GPR) ↓: superior temporal gyrus, cerebellum (ALE), precuneus, dorsal lateral prefrontal cortex, lateral occipital region (GPR)

Ma, 2015 [b]	22	SSRI, SNRI	fMRI (emotional processing)	ALE, FDR-corrected, GingerALE 2.3	↑: dorsolateral prefrontal cortex (negative emotions) ↓: amygdala, hypothalamus, putamen, middle temporal gyrus, ventromedial prefrontal cortex, posterior insula, middle frontal gyrus (negative emotions) ↑↓: amygdala, dorsolateral prefrontal cortex, hippocampus, ventromedial prefrontal cortex, anterior cingulate cortex, fusiform, anterior insula, precuneus (positive emotions)
Boccia et al., 2016	12	Antidepressants, Psychotherapy	fMRI	ALE, FDR-corrected, GingerALE 2.1	↑↓: insula, anterior cingulate cortex, precentral and postcentral gyri, middle frontal gyrus, precuneus, basal ganglia, putamen, cerebellum
Chau et al., 2017	7	SSRI, TMS, ECT	PET, SPECT, ASL-fMRI (resting-state)	MLKD, cFWE-corrected	↑: - ↓: anterior insula
Li et al., 2022[c]	33	Antidepressants (incl. ketamine), CBT, ECT	fMRI, PET, VBM	ALE, cFWE-corrected, GingerALE 3.0	↑: amygdala, parahippocampal gyrus, thalamus ↑↓: amygdala, parahippocampal gyrus, thalamus, anterior cingulate cortex, middle frontal gyrus, insula, claustrum
Current paper	37	Antidepressants (incl. ketamine)	fMRI, PET, SPECT	ALE, cFWE-corrected, pyALE	↑: dorsolateral prefrontal cortex ↓: - ↑↓: -

[a] Only includes number of studies on the effects of pharmacotherapy on MDD, excluding other treatments and disorders, [b] Reported results indicate antidepressant effects in mood disorders including depression and anxiety. Results specific to MDD were not reported. [c] Reported results indicate effects of all treatments. Specific effects of antidepressant medications were not reported.

↑: increased imaging measures, ↓: decreased imaging measures, ↑↓: changed imaging measure in any direction , SSRI: selective serotonin reuptake inhibitor, SNRI: serotonin-norepinephrine reuptake inhibitor, TMS: transcranial magnetic stimulation, CBT: cognitive behavioral therapy ECT: electroconvulsive therapy, PET: positron emission tomography, SPECT: single-photon emission computed tomography, fMRI: functional magnetic resonance imaging, ASL: arterial spin labeling, VBM: voxel-based morphometry, ALE: activation likelihood estimation, FDR: false discovery rate, MKLD: cFWE: cluster-level family-wise error correction, multilevel kernel density.